Célia Maria Lago Pedro

Simulation and NMPC of PET Esterifier

2016

· U C ·

UNIVERSIDADE DE COIMBRA

University of Coimbra

Faculty of Sciences and Technology

Department of Chemical Engineering

Simulation and NMPC of PET Esterifier

Master Thersis in Chemical Engineering, supervised by Doctor Ana Sofia Ramos Brásio and Doctor Lino de Oliveira Santos and submitted to the Department of Chemical Engineering, Faculty of Science and Technology, University of Coimbra.

Célia Maria Lago Pedro

celiapedro92@gmail.com

Coimbra

2016

AOS MEUS PAIS E AOS MEUS IRMÃOS

Acknowledgements

Abstract

This dissertation contributes to the modelling, simulation, and control of the primary esterifier reactor present in the polyethylene terephthalate production process by terephthalic acid based technology.

Polyethylene terephthalate, commonly known as PET or PETE, has globally one of the biggest production volumes in the polymer industry that has enjoyed continuous investment due to its versatility, low cost, and environmental friendliness. PET is mainly obtained by TPA (terephthalic acid) based technology via a continuous complex polymerisation process comprising several stages whose mathematical modelling is not a trivial task. The primary esterifier is the first stage where PET formation occurs. This process features several side reactions producing chemicals with a big negative impact on the final product quality.

The present work has resulted in three applications of the primary esterifier model. The first application consists of a batch reactor simulator that implements a complete segment-based primary esterifier model proposed by Seavey and Liu (2009) and that incorporates a kinetic model for the direct esterification reaction of the ethylene glycol and terephthalic acid. The software was written in GNU Octave. For validation purposes, a case study of the batch reactor start-up showed that the simulated results are in agreement with the data obtained from the Fortran numerical implementation by Seavey and Liu (2009).

In the second application, the reaction kinetic model was introduced into a dynamic continuous esterifier simulator considering vapour, liquid, and solid phases, as in Seavey and Liu (2009). In this dissertation, to enable the use of the model in real-time optimisation tools such as advanced process control, the discontinuous structures of the dynamic model were smoothed out using two different smoothing approaches. The resulting continuous process simulator, also implemented in GNU Octave, was used in the case study of the reactor start-up. The dynamic profiles show a good agreement with the results of Seavey and Liu (2009), although minor differences were observed near the points were the switching between different model structures occurs because of the application of the smoothing functions. Furthermore, a study on the

operating conditions was accomplished for ratios between feed ethylene glycol and total feed mass flowrates in the ranges of [0.1, 0.9] and for temperatures in the range of [246, 286]°C. The influence on conversion, intrinsic viscosity, molar PET production rate, and number-average molecular weight confirmed the strong nonlinear behaviour of the esterifier dynamic model.

Finally, the third application is a nonlinear predictive controller, implemented using the Plantegrity® system, with the purpose of the optimisation of the PET primary esterifier operation. In the process of the controller construction, the nonlinear first principle model was translated to C++, the core language of Plantegrity®. Several tests were carried out in order to demonstrate the system capabilities of performing regulatory and servo control. The controller determined successfully the optimal profiles of the process variables improving the process economic performance while complying with the final product specifications.

Keywords: PET production process, primary esterifier, direct esterification reaction, modelling, simulation, control, model predictive control, Plantegrity® system.

Resumo

O principal objetivo desta dissertação consiste na modelação, simulação e controlo de um reator primário de esterificação presente no processo de produção de politereftalato de etileno, pela tecnologia baseada no ácido tereftálico.

A produção de politereftalato de etileno, mais conhecido por PET ou PETE, é considerada uma das maiores indústrias na área dos polímeros. O PET é um material versátil, de baixo custo e amigo do ambiente e, por isso, os seus produtores têm realizado um constante investimento na melhoria do seu processo produtivo ao longo dos anos. O PET é produzido maioritariamente a partir da reacção entre o ácido tereftálico (TPA) e o etileno glicol (EG) através de um processo complexo de polimerização composto por várias etapas cuja modelaçã matemática não é trivial. O reator primário de esterificação é a primeira etapa onde se forma o PET apresentando várias reações secundárias das quais resultam compostos não desejáveis que prejudicam a qualidade do produto final.

Do presente trabalho resultaram três aplicações do modelo do reator primário de esterificação. A primeira aplicação consistiu no desenvolvimento de um simulador de um reator decontínuo que implementa numericamente o modelo de Seavey and Liu (2009), baseado nos segmentos presentes na molécula de PET. Este modelo incorpora o modelo cinético da reacção directa de esterificação do ácido tereftálico e do etileno glicol. A implementação numérica foi realizada em GNU Octave. Para efeitos de validação da implementação em GNU Octave, simulou-se o arranque do reator descontínuo. Os perfis de simulação são concordantes com os resultados da implementação numérica em Fortran de Seavey and Liu (2009).

Numa segunda aplicação, o modelo cinético foi introduzido num simulador de um esterificador contínuo dinâmico em que são consideradas as fases sólida, liquída e de vapor tal como em Seavey and Liu (2009). Nesta dissertação, para poder aplicar o modelo no contexto de controlo avançado de processos, as estruturas do modelo de caracter descontínuo foram suavizadas recorrendo a duas abordagens de suavização. O simulador foi desenvolvido recorrendo à liguagem de programação GNU Octave. Os resultados de simulação do arranque do reator são concordantes com os perfis de-

terminados por Seavey and Liu (2009), com pequenas diferençãs observadas na vizinhança de pontos de operação em que se verifica as descontinuidades no modelo original. Para além disso, um estudo das condições operatórias foi realizado para razões mássicas entre os caudais de EG e TPA na gama [0.1, 0.9] e para temperaturas na gama [246, 286]°C. A análise da variação da conversão, viscosidade intrínseca, produção molar de PET e peso molecular médio numérico permite concluir que o reator exibe um comportamento não-linear muito pronunciado.

Finalmente, na terceira aplicação desenvolveu-se um controlador preditivo baseado em modelos não-lineares (NMPC) usando o sistema Plantegrity® de modo a otimizar a operação do reator primário de esterificação. Para poder-se desenvolver NMPC neste sistema foi necessário implementar o modelo do reator contínuo na linguagem de programação C++ por ser a linguagem base do sistema Plantegrity®. Foram realizados diferentes testes, em ciclo fechado, para demonstrar o desempenho do NMPC quer em controlo regulador, quer em controlo servo. O controlador determinou com sucesso os perfis ótimos das variáveis do processo, com o consequente melhoramento do desempenho económico do reator e satisfazendo as especificações do produto final.

Keywords: Processo de produção de PET, reator primário de esterificação, modelação, simulação, controlo, controlo preditivo baseado em modelos, sistema Plantegrity®.

Contents

List of Figures

List of Tables

Nomenclature

Symbol	Description	Units
A	interfacial area	m^2
C	concentration	mol m^{-3}
d	degree of polymerisation	dimensionless
D	molecular diffusivity	$\text{m}^2\,\text{s}^{-1}$
E_a	activation energy	J mol^{-1}
f	differentiable real function	dimensionless
F	molar flowrate	mol s^{-1}
$\widetilde{f}$	smoothed function	dimensionless
g	real function	dimensionless
G	species interaction	mol s^{-1}
IV	intrinsic viscosity	dL g^{-1}
k	reaction rate constant	$\text{m}^3\,\text{mol}^{-1}\,\text{s}^{-1}$
K	equilibrium constant	dimensionless
k_0	pre-exponential factor	$\text{m}^3\,\text{mol}^{-1}\,\text{s}^{-1}$
k_s	TPA mass-transfer coefficient	m s^{-1}
$\dot{m}$	mass flowrate	kg s^{-1}
MW	molecular weight	kg mol^{-1}
MW_N	number-average molecular weight	$\text{kg mol}^{-1\star}$
n	mass transfer flux	$\text{mol m}^{-2}\,\text{s}^{-1}$
N	molar holdup	mol
P	pressure	Pa
P^sat	vapour pressure of pure species	Pa
r	generation reaction rate	$\text{mol m}^3\,\text{s}^{-1}$
R	ideal gas constant	$\text{J K}^{-1}\,\text{mol}^{-1}$

R_{EG}	ratio between feed EG and total feed mass flowrates	m/m
t	time	s
t_{c}	average contact time	s
T	temperature	$\mathrm{K}^{\star}$
v	liquid molar volume	$\mathrm{m}^3\,\mathrm{mol}^{-1}$
V	phase volume	m^3
w	liquid phase mass fraction	m/m
x	liquid phase molar fraction	n/n
X	segment-based mole fraction	n/n
y	vapour phase molar fraction	n/n
Y	segments concentration	$\mathrm{mol}\,\mathrm{m}^{-3}$
z	solid phase molar fraction	n/n

Greek letters:

α	solid TPA solubility	$\mathrm{mol}\,\mathrm{m}^{-3}$
ρ	liquid density	$\mathrm{kg}\,\mathrm{m}^{-3}$
γ	activity coefficient	dimensionless
ΔH	heat of reaction	$\mathrm{J}\,\mathrm{mol}^{-1}$
ν	molar volume	$\mathrm{kmol}\,\mathrm{m}^{-3}$
ξ	accuracy parameter	dimensionless
τ	interaction parameter	dimensionless
ϕ	segment-based mole fraction dependent variable	n/n
$\varphi_{\mathrm{liq-sol}}$	weir constant	$\mathrm{mol}\,\mathrm{s}^{-1}\,\mathrm{m}^{-\frac{9}{2}}$
φ_{vap}	vapour phase flow constant	$\mathrm{mol}\,\mathrm{s}^{-1}\,\mathrm{Pa}^{-0.5}$
χ	conversion	$\%(m/m)$
$\mathcal{H}$	Heaviside function	dimensionless
$\widetilde{\mathcal{H}}$	smoothed Heaviside function	dimensionless
ς	randomness factor	dimensionless
ξ	correction constant	dimensionless
λ_l	weighting scalars	dimensionless

Acronyms:

AA	Acetaldehyde
BHET	Bis-2-hydroxilethyl-terephthalate
B-DEG	Diethylene glycol segment
B-EG	Ethylene glycol segment
B-TPA	Terephthalic acid segment
DCS	Distributed control system
DEG	Diethylene glycol
DMT	Dimethyl terephthalate
EG	Ethylene glycol
LB	Lowerbound
LRB	Lowerratebound
PET	Polyethylene terephthalate
PLC	Programmable logic controller
TPA	Terephthalic acid
T-EG	Ethylene glycol terminal
T-TPA	Terephthalic acid terminal
T-VIN	Vinyl terminal
T-DEG	Diethylene glycol terminal
UB	Upperbound
URB	Upperratebound
W	Water

Subscripts:

FH	Florry-Huggins
in	inlet
liq	liquid phase
NRTL	non-random two liquid
out	outlet
p	polymer
s	solvent
sol	solid phase
vap	vapour phase

* When explicitly stated, $\mathrm{MW_N}$ and T may also be expressed in g mol^{-1} and $^\mathrm{o}$C, respectively.

Chapter 1

Introduction

This chapter describes and justifies the objective of this thesis and explains the way how it is organised. Finally, a review of the literature needed to the understanding of the study carried out in this work is covered.

1.1 Scope and Motivation

Polyethylene terephthalate, or PET as commonly is abbreviated, has been widely used in the recent decades (Bartolome et al., 2012) because of its low cost, excellent tensile strength, chemical resistance, clarity, processability, and reasonable thermal stability. In fact, it is one of the most important man-made fibres and the market demands tight property specifications and an extensive stock management due to its applications diversity. Two of the important polymer properties are the molecular weight (a measure of the polymeric chain size) and the intrinsic viscosity (a measure of the PET molecules contribution to the solution viscosity) that define the exact specification of the final product (Seavey and Liu, 2009; Plastics Industry Trade Association, 2016).

Industrially, PET is obtained mainly via a continuous complex polymerisation process that involves terephthalic acid and ethylene glycol and that comprises several stages: primary and secondary esterification, low, intermediate, high and solid state polymerisation. The polymerisation reaction occurring in the first four stages is characterised by a strong nonlinear behaviour which is one of the most challenging problems in the PET production process. The modelling of this process is not trivial and a variety of works that deal with the issue have been reported in the literature (Mazloom et al., 2007; Manenti and Rovaglio, 2008; Immanuel, 2000). It is note-

worthy that there are several side reactions producing chemicals that have an enormous impact on the final product quality and that must be carefully monitored. It is the case of diethylene glycol, acetaldehyde, and vinyl end groups. In the early stages of PET synthesis, diethylene glycol is the most important side product that incorporates the PET molecules influencing their physical and chemical properties. For instance, the increasing of diethylene glycol content in PET molecules decreases their melting point and crystallisation temperature (Besnoin and Choi, 1989). At the same time, the multilevel production of PET occurs at high temperatures requiring huge amounts of energy (Kim et al., 2001).

Modelling, simulation, and optimisation are important for the economic improvement of the continuous PET production process. For instance, an advanced process control application as an optimisation procedure based on a mathematical model may allow both process and product quality control. In addition, it may be possible to take into account process constraints and to avoid unsteady operation, side product formation, as well as to reduce the specific energy consumption.

Therefore, this thesis focuses on the modelling and optimisation of the primary esterifier that according to Patel et al. (2007b) is considered to be a critical stage of PET production. The present work builds upon previous contributions of Manenti and Rovaglio (2008) and Manenti (2011) in the field.

This work was carried out at Ciengis - Advanced Control Systems company with the goal of studying in detail the PET primary esterifier using mathematical modelling, computational simulation, and optimisation tools in order to optimise the process in terms of product quality and production costs.

1.2 Objectives

In accordance with the above motivations, the objectives are:

- to implement computationally the Seavey and Liu (2009) mathematical model that describes the PET primary esterifier dynamic behaviour based on first principles, in order to be used in the context of process optimisation tools, such as advanced process control. The simulation study focuses on the complex reaction kinetics and the continuous reactor where the esterification reaction between terephthalic acid and ethylene glycol occurs. Using this implementation, a study of the process dynamics and of the operating conditions was carried out.

- to apply nonlinear model process control based on the implemented nonlinear first principle dynamic model in order to optimise in real time the PET primary esterifier in terms of product quality and production costs. In a simulation environment, optimal profiles of the process variables are determined by the Plantegrity® model predictive control system in order to evaluate the closed loop process performance, while complying with product specification and process constraints.

1.3 Thesis Outline

This dissertation is organised in five chapters as well as an appendix containing complementary information.

Chapter 1 presents the scope, motivation and objectives of the work and lays out its theoretical base.

Chapter 2 aims to study the selected reaction kinetic model.

In **Chapter 3**, the continuous esterifier model is detailed together with the main physical and chemical properties. A study of the most important operating conditions is performed in order to understand the optimal operating envelope.

Chapter 4 demonstrates the application of advanced process control using the mathematical model presented in **Chapters 2** and **3**.

Finally, the main conclusions of this work are drawn in **Chapter 5** and suggestions for future work are highlighted.

1.4 State-of-the-art

1.4.1 Polyethylene terephthalate

Plastic is one of the most used materials and its applications ranges from food producers to cars manufactures (IBISWorld, 2016). As Patel et al. (2007b) refers, the global production of PET was about 35 million tons per year in 2007. In USA, for instance, it is the third largest manufacturing industry with around 18,500 plastics facilities serving the USA economy (Plastics Industry Trade Association, 2016). The advantages and versatility of plastics over other similar materials make it such an interesting material that industries operators keep investing in research and development to create low-cost and environmental friendly plastics (IBISWorld,

2016).

Polyethylene terephthalate is a thermoplastic polymer resin that belongs to the polyester family. PET was initially patented in 1941 by John Whinfield and James Dickson in the Calico Printer's Association of Manchester. They worked with others for the creation of the first polyester fibre. The first brand of PET was Terylene realised in 1941 followed by new brands. A later patent was filed by Nathaniel Wyeth, in 1973, for PET bottles but later was decided that could be used for medicine purposes (SRI, 2016).

PET polymer can be found in different forms, from semi-rigid to rigid, depending on the thickness. This material can be transparent or a semi-crystalline polymer. Despite of that, colour can be added if necessary. Its lightness does not prevent it from being a very strong and resistant material. All of these advantages make PET one of the most common plastics nowadays (Todd Johnson, 2016).

Some examples for PET uses are synthetic fibres and the common drink bottles for water, soft drinks, etc. In a form of film, PET can be used for balloons, flexible food packaging space blankets and more. Moreover, it can be combined with other materials to achieve the required properties, for example, if glass particles or fibres are added to PET, it will become more durable and stiffer. According to Patel et al. (2007b), 63 % of produced PET is used in polymer resins, filament and woven forms and 37 % in packaging. Finally, its important to refer that this material can be recycled and used again in a lot of different products (SRI, 2016; Todd Johnson, 2016).

1.4.2 PET production processes

Commercial polyethylene terephthalate is obtain by polycondensation. Currently, PET can be formed by two different processes: based on dimethyl terephthalate (DMT) or on terephthalic acid (TPA).

In DMT based technology, DMT reacts with ethylene glycol (EG) by transesterification reaction to provide bis(2-hydroxyethyl) terephthalate (BHET), which will be the monomer of PET reaction. Total conversion of raw materials is attained after the methanol removal since the reaction is reversible. The monomer is polymerised by polycondensation in order to yield PET (Manenti, 2011).

In TPA based technology, the raw materials are TPA and EG, they react by direct esterification to yield BHET, water and oligomers. Like in DMT based technology, the reactions are

reversible, thus water has to be removed during the reaction. TPA based technology is the most used technology because it allows faster reactions rates and better yields, at the same operating conditions. Moreover, the presence of methanol in the DMT route as a by-product makes the process more hazardous to handle, compared to water in the TPA route. On top of that, TPA based technology represents a 20 % reduction in variable costs (Manenti and Rovaglio, 2008) and allows to operate with EG:TPA ratios of 1:1, in opposition to the 1.8:1 of DMT based technology, producing smaller DEG quantities. DEG is a very important side product, since influences chemical and physical PET properties, whose formation must be controlled. This component influences the final PET properties such as light stability and melting point (Banat and Abu, 2001; Kim et al., 2001).

PET production processes can be continuous or discontinuous. Industrially, a continuous process by TPA based technology is preferred (Figure 1.1). Normally, liquid EG is mixed with solid TPA previously in a tank, forming a paste, and fed to the primary esterifier (PE). Th oligomer formed is send to a second esterifier (SE). This stage is followed by the low polymerisation (LP), responsible for the removal of the extra EG and water in the process. Intermediate and high polymerisation (IP and HP, respectively) are then carried out allowing the melt phase polymerisation to reach the maximum feasible degree (Manenti, 2011). In the last section, the solid state polymerise (SSP) extrudes the solid polymer in pellets following into a moving bed reactor where molecular weight is increased (Manenti, 2011).
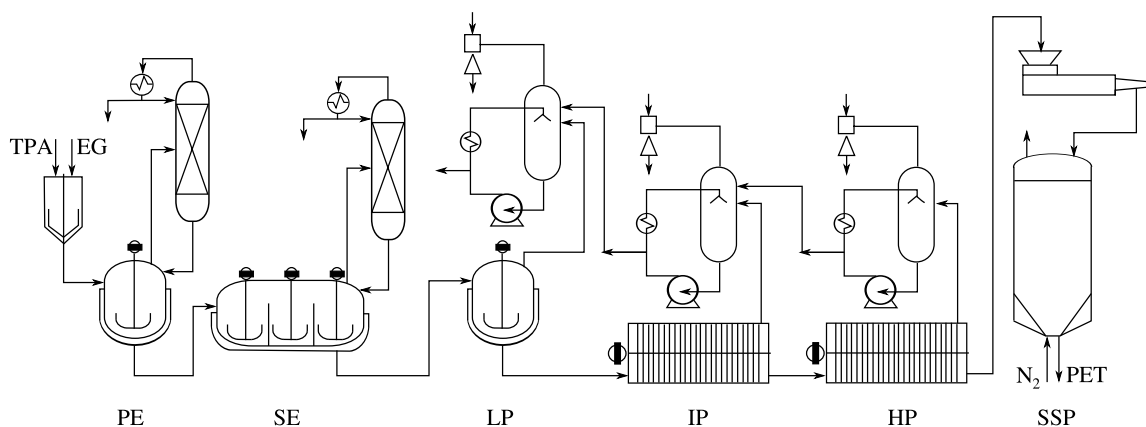

Figure 1.1: Process flow diagram of the TPA based technology. Adapted from Manenti (2011).

1.4.3 Mathematical Modelling

Mathematical modelling is a way of describing various process components, their interaction and their dynamics through mathematical equations (Maria, 1997). This model might be used to predict the process evolution and the result of different experiments without spending economical resources and assuring the process safety. Process optimisation tools usually use developed mathematical models to find optimal operating conditions of the process.

Polymerisation systems models may be classified into two approaches: the species-based and the segment-based models. The species-based models consider the polymer as a single molecule, while the segment-based models consider the polymer repeat unit as an individual molecule. The advantage of the segment-based approach is the possibility of characterising polymer properties by the chemical properties of the segments comprising the polymer molecules (Seavey and Liu, 2009).

Several works are dedicated to the polymerisation reaction existing in the PET production process focused on esterification reaction between TPA and EG. Some work on modelling was done by Kumar and co-workers. In Kumar et al. (1984), a thin film reactor for PET production is modelled including film thickness, surface area, concentration, exposure time, residence time and temperature as design variables. Later, they developed a kinetic model counting for the intermolecular reaction in step-growth polymerisation of multifunctional monomers (Kumar et al., 1986).

Similarly to the Kumar group, Yamada and his co-workers have some work developed in PET process modelling. One of their first contributions is divided into two parts. Part one shows a model of a direct continuous esterifier for PET production using EG and TPA as raw materials (Yamada and Imamura, 1985). This work is focused on the measure of the liquid weight fraction of bis-2-hydroxyethyl terephthalate (BHET) in the reaction mixture. Its prediction can be useful to estimate the concentration of each component. In the second part (Yamada and Imamura, 1986), the kinetic parameters are estimated applying the simplex method to plant data. Later, Yamada presented an optimised model for the direct esterification where he studied the influence of potassium titanium in side reactions (Yamada and Imamura, 1989). This study allowed to estimate the amount of EG and water in liquid mixtures as well as the physical parameters of the system. Later, Yamada and Imamura (1988) focused on the reaction between TPA and EG under reduced pressures. This development allowed the deduction of optimum operating conditions for oligomers production using minimum of the reactant EG.

The continuous direct esterification was also studied in Kang and Ihm (1997) considering the liquid-solid equilibrium. The dissolution of TPA takes into account adjustable parameters and characteristic dissolution time. Immanuel (2000) designs a new model with sequence of three CSTRs in series for the esterification, measuring TPA and EG conversion, product molecular weight and side products concentration. Additionally Chen and Chen (1998) studied the effect of TPA addition at the initial fed stream achieving an optimal point for a feed molar ratio between reactants in the range of 1.0 to 1.3.

In 2001, Kim et al. (2001) proposed a new kinetics reaction model based on the genetic algorithm. He studied the effect of some operating parameters, such as temperature, pressure, monomer, feed ratio and residence time, on the reaction. A two phase system considering solid TPA solubility in liquid phase was focused in Ahn and Choi (2003) based on a set of differential equations obtained from mass balances using the Newton-Raphson method. Later, Mazloom et al. proposed a new mathematical model based on results from a laboratory size unit considering esterification and polycondensation reactions (Mazloom et al., 2007). The model obtained from mass balances resulted in nonlinear ordinary differential equations solved with the Runge-Kutta method.

The literature also presents some work about semi-batch esterification processes. Patel et al. (2007b) studied the reaction kinetics and investigated the influence of TPA particles size distribution in solid-liquid mass-transfer. Following Yamada and Imamura (1988) work, the same authors presented a study about the lower pressures influence in semi-batch PET esterifier (Patel et al., 2007a). The solid-liquid equilibrium was considered during the study of the temperature effect and mass feed ratio fed in Kang et al. (1996).

Luo and Qian (2012) proposed an approach to determine the kinetic parameters using the multi-objective estimation of distribution algorithm.

1.4.4 Process Optimisation via Advanced Process Control

PET process optimisation can reduce economic costs while product quality and operation constraints are satisfied. PET quality specification is rather tight which calls for a highly performing process control. Nowadays, industries mainly resort to linear model process control even thought some dynamic nonlinear models have been developed (Manenti, 2011).

In accordance with Manenti and Rovaglio (2008), the increased profit by opting for a dynamic nonlinear model in optimisation tools is about $12.5 million per year and 1 month of

payback. Therefore, the application of nonlinear model process control based on a dynamic nonlinear plant model seems to be an appropriate solution (Manenti and Rovaglio, 2008).

Nonlinear model process control (NMPC) with origin in the 70's is an advanced process control technology which implements a process model and an algorithm to determine optimal profiles for the manipulated variables by minimising an objective function (Allgöwer et al., 2004). Systems with multiple inputs and outputs can be handled naturally by NMPC together with process constrains (Maca, 2005). In that work, NMPC technology based on a first principle model is applied by simulation to control an esterifier reactor. The integration of a NMPC control strategy in this reactor was first performed in Manenti and Rovaglio (2008). In this work, the process design includes esterifiers section, finishers section, a crystalliser and a solid state polymerise. The mathematical model is composed by more than 1500 differential and algebraic equations implemented using both Windows and Unix operating systems. For the primary esterifier, they considered a temperature range between 530 and 555 K and a pressure between 2 and 8 atm. The equipment is modelled as a continuous reactor where the kinetics schemes of Kang and Ihm (1997) and Kim et al. (2003) are used. The vapour-liquid equilibrium is also considered using Flory-Huggins correlation equations. The chosen control scheme for the PET esterifier defines the reactor temperature and pressure as controlled variables, and EG flowrate, the ratio between liquid EG and solid TPA flowrate, wall temperature, and discharged pressure as manipulated variables.

Other work in this area was developed by the same group in Manenti (2011) where an appealing variant of NMPC ensures a reasonably efficient and a robust solution of the controller that is applied using the same control scheme. According to the author, this new variant is able to self-select the algorithms that are used for the specific problem, conferring high levels of generality and flexibility of the control strategy.

Chapter 2

Modelling of Reaction Kinetics

This chapter describes the implementation of a kinetic model of the direct esterification reactions and its incorporation into a batch esterification reactor model. The latter is used in a case study of reactor start-up and the obtained results are compared with the literature. The effect of the most important polymer properties is explored.

2.1 Direct Esterification Reaction

The reactants used in the esterification unit are liquid ethylene glycol (EG) and solid terephthalic acid (TPA) as Figure 2.1 depicts. A reaction via direct esterification mechanism of TPA produces polyethylene terephthalate (PET), water (W), diethylene glycol (DEG) and acetaldehyde (AA) as the main products. Solid TPA, liquid TPA, and liquid EG are also present in the final reaction mixture.
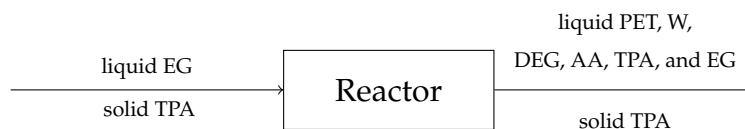
Figure 2.1: Reactor inlet and outlet components.

Since all the reactions occurs simultaneously, a complex scheme of parallel and side reactions has to be considered together with the equilibrium between the two phases (Scheirs and Long, 2003). The considered model is based in the reaction scheme and kinetics described in Seavey and Liu (2009) work.

9

PET reaction mechanism is characterised by two principal reactions (Seavey and Liu, 2009):

1. water formation where alcohol reacts with carboxylic acid producing ester and water, and

2. ester interchange where an ester reacts with other rearranging the groups.

The approach of Seavey and Liu (2009) considers that PET chain is composed by different oligomers formed in the several reactions classified into bounded (B-) and terminal (T-) groups. The bounded oligomers are B-DEG, B-EG, and B-TPA and the terminal oligomers are T-DEG, T-EG, T-TPA, and T-VIN. The functional groups, the oligomers associated to this reaction and their molecular structure are shown in detail in Table 2.1.

The two main reactions are followed by side reactions. Degradation of diester group, formation of T-DEG and B-DEG, the dehydration of EG and T-EG, and last but not least the AA formation (Seavey and Liu, 2009). During direct esterification, the most important side product formed is DEG, produced in its first stages. The other side products are formed mainly in the last stages of the esterifier. Since the amount of DEG in the reaction mixture influences physical and chemical properties, the predictions of its exact concentration is very important in the reactor modelling (Kim et al., 2001). Carboxylic groups and acetaldehyde, are the components that can lead to problems of quality and discolouration of the product. Therefore, the operating temperature side reactions dependency will contribute to a better PET quality by controlling it (Kim et al., 2003).

The reaction steps considered are (Seavey and Liu, 2009):

Step 1 Esterification
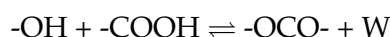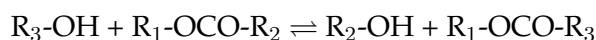
-OH + -COOH $\rightleftharpoons$ -OCO- + W

Step 2 Ester interchange

R_3-OH + R_1-OCO-R_2 $\rightleftharpoons$ R_2-OH + R_1-OCO-R_3

Step 3 Degradation of diester

B-TPA:B-EG $\rightarrow$ T-VIN + T-TPA

Step 4 DEG formation

B-TPA:B-EG + T-EG $\rightarrow$ B-TPA:T-DEG

T-VIN + T-EG $\rightarrow$ B-DEG
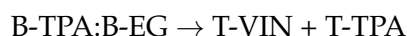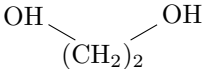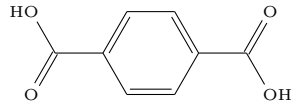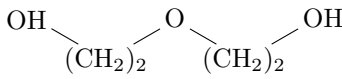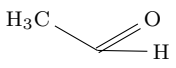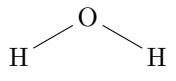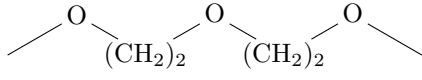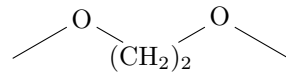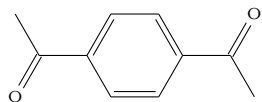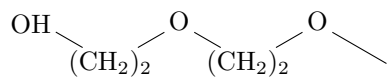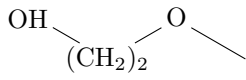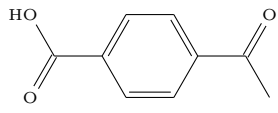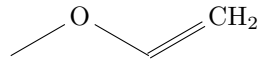
Table 2.1: Segment names and formulas of the considered oligomers.

Species	Description	Chemical Formula	Molecular Structure
EG	Ethylene glycol	$C_2H_6O_2$	
TPA	Terephthalic acid	$C_8H_6O_4$	
DEG	Diethylene glycol	$C_4H_{10}O_3$	
AA	Acethaldeyde	C_2H_4O	
W	Water	H_2O	
B-DEG	DEG repeat segment	$C_2H_8O_3$	
B-EG	EG repeat segment	$C_2H_4O_2$	
B-TPA	TPA repeat segment	$C_8H_2O_2$	
T-DEG	DEG end group	$C_4H_9O_3$	
T-EG	EG end group	$C_2H_5O_2$	
T-TPA	TPA end group	$C_8H_2O_2$	
T-VIN	Vinyl end group	C_2H_3O	

Step 5 EG dehydration

T-EG + T-EG → B-DEG + W

T-EG + EG → T-DEG + W

Step 6 AA formation

B-TPA:T-EG → AA+ T-TPA
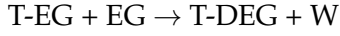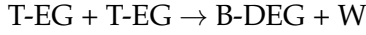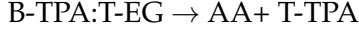
2.2   Mathematical Modelling

Considering the segment-based Seavey and Liu (2009) model, the material balance equation of each component and segment in the liquid phase of the batch reactor is written as[1]

$$\frac{dC_{AA}}{dt} = r_8 + r_{10} + \sum_{j=23}^{30} r_j + r_{37} \; , \tag{2.1}$$

$$\frac{dC_{B\text{-}DEG}}{dt} = r_7 + r_8 - r_{13} - r_{16} - r_{19} - r_{22} + r_{29} + r_{30} + r_{33} + r_{34} \; , \tag{2.2}$$

$$\frac{dC_{B\text{-}EG}}{dt} = r_5 + r_6 - r_{11} - r_{14} - r_{18} - r_{21} + r_{27} + r_{28} - r_{31} \; , \tag{2.3}$$

$$\frac{dC_{B\text{-}TPA}}{dt} = r_2 + r_4 + r_6 + r_8 - r_{10} - r_{31} - r_{32} - r_{37} \; , \tag{2.4}$$

$$\frac{dC_{DEG}}{dt} = -r_3 - r_4 + r_{12} + r_{15} - \sum_{j=17}^{22} r_j - r_{25} - r_{26} + r_{36} \; , \tag{2.5}$$

$$\frac{dC_{EG}}{dt} = -r_1 - r_2 - \sum_{j=11}^{16} r_j + r_{17} + r_{20} - r_{23} - r_{24} - r_{35} - 2r_{36} \; , \tag{2.6}$$

$$\frac{dC_{T\text{-}DEG}}{dt} = r_3 + r_4 - r_7 - r_8 - r_{12} + r_{13} - r_{15} + r_{16} + \sum_{j=17}^{22} r_j + r_{25} \; , \tag{2.7}$$

$$\begin{aligned}
\frac{dC_{T\text{-}EG}}{dt} &= r_1 + r_2 - r_5 - r_6 + 2(r_{11} + r_{14}) + r_{12} + r_{13} + r_{15} + r_{16} \\
&\quad - r_{17} + r_{18} - r_{35} - r_{37} - r_{20} + r_{21} + r_{23} + r_{24} - r_{27} \\
&\quad - r_{28} - 2r_{32} - r_{33} - 2r_{34} \; ,
\end{aligned} \tag{2.8}$$

---

[1]For the sake of nomenclature simplicity, the liquid phase is considered by default. If the variable is considered in the solid phase, it is referred unabbreviated or with the subscript $_{sol}$.

$$\frac{\mathrm{d}C_{\mathrm{TPA}}}{\mathrm{d}t} = -r_1 - r_3 - r_5 - r_7 + r_9 \ , \tag{2.9}$$

$$\frac{\mathrm{d}C_{\mathrm{T\text{-}TPA}}}{\mathrm{d}t} = r_1 - r_2 + r_3 - r_4 + r_5 - r_6 + r_7 - r_8 - r_9 + r_{10}$$
$$+ r_{31} + r_{32} + r_{37} \ , \tag{2.10}$$

$$\frac{\mathrm{d}C_{\mathrm{T\text{-}VIN}}}{\mathrm{d}t} = -r_9 - r_{10} - \sum_{j=23}^{30} r_j + r_{31} - r_{33} \ , \tag{2.11}$$

$$\frac{\mathrm{d}C_{\mathrm{W}}}{\mathrm{d}t} = \sum_{j=1}^{8} r_j - r_9 - r_{10} + \sum_{j=34}^{36} r_j \ , \tag{2.12}$$

where r_j is the generation reaction rate of the j reaction in mol m^{-3} s^{-1} defined as

Step 1: Esterification

1   EG + TPA $\rightleftharpoons$ T-EG + T-TPA + W $r_1 = 4k_1 C_{\mathrm{EG}} C_{\mathrm{TPA}} - k_1/K_1 \ Y_1 C_W$

2   EG + T-TPA $\rightleftharpoons$ T-EG + B-TPA + W $r_2 = 2k_1 C_{\mathrm{EG}} C_{\mathrm{T\text{-}TPA}} - k_1/K_1 \ Y_2 C_W$

3   DEG + TPA $\rightleftharpoons$ T-DEG + T-TPA + W $r_3 = 4k_1 C_{\mathrm{DEG}} C_{\mathrm{TPA}} - k_1/K_1 \ Y_7 C_W$

4   DEG + T-TPA $\rightleftharpoons$ T-DEG + T-TPA + W $r_4 = 2k_1 C_{\mathrm{DEG}} C_{\mathrm{T\text{-}TPA}} - k_1/K_1 \ Y_8 C_W$

5   T-EG + TPA $\rightleftharpoons$ B-EG + T-TPA + W $r_5 = 2k_2 C_{\mathrm{T\text{-}EG}} C_{\mathrm{TPA}} - k_1/K_1 \ Y_3 C_W$

6   T-EG + T-TPA $\rightleftharpoons$ B-EG + B-TPA + W $r_6 = k_2 C_{\mathrm{T\text{-}EG}} C_{\mathrm{T\text{-}TPA}} - k_1/K_1 \ Y_4 C_W$

7   T-DEG + TPA $\rightleftharpoons$ B-DEG + T-TPA + W $r_7 = 2k_2 C_{\mathrm{T\text{-}DEG}} C_{\mathrm{TPA}} - k_1/K_1 \ Y_{10} C_W$

8   T-DEG + T-TPA $\rightleftharpoons$ B-DEG + B-TPA + W $r_8 = k_2 C_{\mathrm{T\text{-}DEG}} C_{\mathrm{T\text{-}TPA}} - k_1/K_1 \ Y_9 C_W$

9   T-VIN + T-TPA + W $\rightarrow$ AA + TPA $r_9 = k_1/K_1 \ Y_6 C_W$

10 T-VIN + B-TPA + W $\rightarrow$ AA + TPA $r_{10} = k_1/K_1 \ Y_5 C_W$

Step 2: Ester interchange

11 EG + B-EG $\rightleftharpoons$ T-EG + T-EG $r_{11} = 2k_3 C_{\mathrm{EG}} Y_3 - k_3/K_3 \ C_{\mathrm{T\text{-}EG}} \ Y_1$

12 EG + T-DEG $\rightleftharpoons$ DEG + T-EG $r_{12} = 2k_3 C_{\mathrm{EG}} Y_7 - 2k_3/K_3 \ C_{\mathrm{DEG}} \ Y_1$

13

13   EG + B-DEG $\rightleftharpoons$ T-DEG + T-EG $r_{13} = 2k_3 C_{\text{EG}} Y_{10} - {k_3}/{K_3}\, C_{\text{T-DEG}}\, Y_1$

14   EG + B-EG $\rightleftharpoons$ T-EG + T-EG $r_{14} = 2k_3 C_{\text{EG}} Y_4 - 2{k_3}/{K_3}\, C_{\text{DEG}}\, Y_2$

15   EG + T-DEG $\rightleftharpoons$ DEG + T-EG $r_{15} = 2k_3 C_{\text{EG}} Y_8 - 2{k_3}/{K_3}\, C_{\text{DEG}}\, Y_2$

16   EG + B-DEG $\rightleftharpoons$ T-DEG + T-EG $r_{16} = 2k_3 C_{\text{EG}} Y_9 - {k_3}/{K_3}\, C_{\text{DEG}}\, Y_2$

17   DEG + T-EG $\rightleftharpoons$ EG + T-DEG $r_{17} = 2k_3 C_{\text{DEG}} Y_1 - 2{k_3}/{K_3}\, C_{\text{EG}}\, Y_7$

18   DEG + B-EG $\rightleftharpoons$ T-EG + T-DEG $r_{18} = 2k_3 C_{\text{DEG}} Y_3 - {k_3}/{K_3}\, C_{\text{T-EG}}\, Y_7$

19   DEG + B-DEG $\rightleftharpoons$ T-DEG + T-DEG $r_{19} = 2k_3 C_{\text{DEG}} Y_{10} - {k_3}/{K_3}\, C_{\text{T-DEG}}\, Y_7$

20   DEG + T-EG $\rightleftharpoons$ EG + T-DEG $r_{20} = 2k_3 C_{\text{DEG}} \cdot Y_2 - {k_3}/{K_3}\, C_{\text{T-DEG}}\, Y_8$

21   DEG + B-DEG $\rightleftharpoons$ T-EG + T-DEG $r_{21} = 2k_3 C_{\text{DEG}} \cdot Y_4 - {k_3}/{K_3}\, C_{\text{T-EG}}\, Y_8$

22   DEG + B-DEG $\rightleftharpoons$ T-DEG + T-DEG $r_{22} = 2k_3 C_{\text{DEG}} \cdot Y_9 - {k_3}/{K_3}\, C_{\text{T-DEG}}\, Y_8$

23   EG + T-VIN $\rightarrow$ AA + T-EG $r_{23} = 2k_3 C_{\text{EG}} \cdot Y_6$

24   EG + T-VIN $\rightarrow$ AA + T-EG $r_{24} = 2k_3 C_{\text{EG}} \cdot Y_5$

25   DEG + T-VIN $\rightarrow$ AA + T-DEG $r_{25} = 2k_3 C_{\text{DEG}} \cdot Y_6$

26   DEG + T-VIN $\rightarrow$ AA + T-DEG $r_{26} = 2k_3 C_{\text{DEG}} \cdot Y_5$

27   T-EG + T-VIN $\rightarrow$ AA + B-EG $r_{27} = k_3 C_{\text{T-EG}} \cdot Y_6$

28   T-EG + T-VIN $\rightarrow$ AA + B-EG $r_{28} = k_3 C_{\text{T-EG}} \cdot Y_5$

29   T-DEG + T-VIN $\rightarrow$ AA + B-DEG $r_{29} = k_3 C_{\text{T-DEG}} \cdot Y_6$

30   T-DEG + T-VIN $\rightarrow$ AA + B-DEG $r_{30} = k_3 C_{\text{T-DEG}} \cdot Y_5$

Step 3: Degradation of diester

31   B-TPA + B-EG $\rightarrow$ T-VIN + T-TPA $r_{31} = k_4 Y_4$

Step 4: DEG formation

32   B-TPA + T-EG + T-EG $\rightarrow$ T-TPA + T-DEG $r_{32} = k_5 Y_2 \cdot C_{\text{T-EG}}$

33 T-VIN + T-EG → B-DEG $\qquad r_{33} = k_6 C_{\text{T-VIN}} \cdot C_{\text{T-EG}}$

Step 5: EG dehydration

34 2 T-EG → B-DEG + W $\qquad r_{34} = k_7 \left(C_{\text{T-EG}}\right)^2 \cdot Y_5$

35 T-EG + EG → T-DEG + W $\qquad r_{35} = 2k_7 C_{\text{T-EG}} \cdot C_{\text{EG}}$

36 2EG → DEG + W $\qquad r_{36} = 4k_7 C_{\text{EG}}^2$

Step 6: AA formation

37 B-TPA + T-EG → AA + T-TPA $\qquad r_{37} = k_8 C_{\text{T-DEG}} \cdot Y_2$
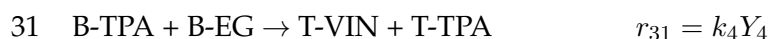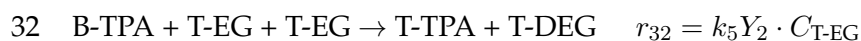
where C_i is the molar concentration of the component i, and Y_i is the segment concentration calculated using

$$Y_1 = C_{\text{T-EG}}\frac{C_{\text{T-TPA}}}{C_{\text{T-TPA}}+C_{\text{B-TPA}}} \quad , \quad Y_2 = C_{\text{T-EG}}\frac{C_{\text{B-TPA}}}{C_{\text{T-TPA}}+C_{\text{B-TPA}}} \quad , \quad Y_3 = C_{\text{B-EG}}\frac{C_{\text{T-TPA}}}{C_{\text{T-TPA}}+C_{\text{B-TPA}}}$$

$$Y_4 = C_{\text{B-EG}}\frac{C_{\text{B-TPA}}}{C_{\text{T-TPA}}+C_{\text{B-TPA}}} \quad , \quad Y_5 = C_{\text{T-VIN}}\frac{C_{\text{B-TPA}}}{C_{\text{T-TPA}}+C_{\text{B-TPA}}} \quad , \quad Y_6 = C_{\text{T-VIN}}\frac{C_{\text{T-TPA}}}{C_{\text{T-TPA}}+C_{\text{B-TPA}}}$$

$$Y_7 = C_{\text{T-DEG}}\frac{C_{\text{T-TPA}}}{C_{\text{T-TPA}}+C_{\text{B-TPA}}} \quad , \quad Y_8 = C_{\text{T-DEG}}\frac{C_{\text{B-TPA}}}{C_{\text{T-TPA}}+C_{\text{B-TPA}}} \quad , \quad Y_9 = C_{\text{B-DEG}}\frac{C_{\text{B-TPA}}}{C_{\text{T-TPA}}+C_{\text{B-TPA}}}$$

$$Y_{10} = C_{\text{B-DEG}}\frac{C_{\text{T-TPA}}}{C_{\text{T-TPA}}+C_{\text{B-TPA}}} \ .$$

The conversion between molar concentration derivatives and molar holdup derivatives is obtained by

$$\frac{\mathrm{d}N_i}{\mathrm{d}t} = \frac{\mathrm{d}C_i}{\mathrm{d}t}V_{\text{liq}}, \tag{2.13}$$

where V_{liq} is the liquid phase volume in m^3 and t the time in s.

Considering the equilibrium between solid and liquid phases and solid TPA dissolution, the mass balance to the liquid TPA can be written as

$$\frac{\mathrm{d}N_{\text{TPA}}}{\mathrm{d}t} = (-r_1 - r_3 - r_5 - r_7 + r_9 + r_{10})V_{\text{liq}} + k_{\text{s}}\, A_{\text{sol}-\text{liq}}\left(\alpha - C_{\text{TPA}}\right), \tag{2.14}$$

where $A_{\text{sol}-\text{liq}}$ is the solid-liquid interfacial area in m^2, α the solubility of TPA in the liquid mixture in mol m^{-3}, C_{TPA} the TPA concentration in the liquid phase in mol m^{-3}, and k_{s} the mass transfer coefficient in m s^{-1}.

The mass balance to the TPA in the solid phase is obtained by

$$\frac{\mathrm{d}N_{\text{sol,TPA}}}{\mathrm{d}t} = -k_{\text{s}} \, A_{\text{sol−liq}} \, (\alpha - C_{\text{TPA}}) \,. \tag{2.15}$$

Due to the lower solubility of solid TPA in liquid EG (Kang et al., 1996; Seavey and Liu, 2009), the concentration of the dissolved TPA in the liquid phase is considered to be in the solid-liquid equilibrium. The TPA solubility is then given by (Kang et al., 1996; Seavey and Liu, 2009)

$$\alpha = \alpha_{\text{EG}} w_{\text{EG}} + \alpha_{\text{BHET}} w_{\text{BHET}} \,, \tag{2.16}$$

where α_{EG} and α_{BHET} are the solubilities of TPA in EG (mol TPA/kg EG) and in BHET (mol TPA/kg BHET), respectively, and w_{EG} and w_{BHET} are EG and BHET mass fractions (m/m), respectively. These variables are described mathematically by (Seavey and Liu, 2009; Kang et al., 1996)

$$\alpha_{\text{EG}} = 9062 \exp\left(-\frac{4877}{T}\right) \,, \tag{2.17}$$

$$\alpha_{\text{BHET}} = 374 \exp\left(-\frac{3831}{T}\right) \,, \tag{2.18}$$

where T is the mixture temperature in K. It is considered that TPA solubility in other components is negligible (Seavey and Liu, 2009).

The kinetics study considering the antimony triacetate, SBOAC$_3$, catalyst defines the overall reaction rates as (Bhaskar et al., 2001)

$$k_i = k_{0,i} \cdot \frac{w_{\text{SBOAC}_3}}{0.0004} \cdot \exp\left(-\frac{E_{\text{a},i}}{R\,T}\right) \,, \tag{2.19}$$

where $k_{0,i}$ represents the pre-exponential factor in m^3 mol^{-1} s^{-1}, w_{SBOAC_3} the mass fraction of SBOAC$_3$ in m/m, $E_{\text{a},i}$ the energy of activation in J mol^{-1}, and R the ideal gas constant in J K^{-1} mol^{-1}. This study is valid for a catalyst concentration lower or equal to $0.04\,\%(m/m)$. Overall reaction rate constants are given in Table 2.2.

To evaluate the polymer quality, it is important to measure two different properties: the number-average molecular weight (MW$_{\text{N}}$) in g m^{-1}, and intrinsic viscosity (IV) in dL g^{-1}, defined by

$$\text{MW}_{\text{N}} = \frac{\sum\limits_{i \in \mathcal{I}} N_i \cdot \text{MW}_i + \sum\limits_{j \in \mathcal{J}} \cdot N_j \text{MW}_j}{^{1\!/\!2} \sum\limits_{j \in \mathcal{J}} N_j} \,, \tag{2.20}$$

Table 2.2: Overall reaction rate constants (Bhaskar et al., 2001).

i	$k_{0,i}$	$E_{a,i}$
	$m^3 \, mol^{-1} \, s^{-1}$	$J \, mol^{-1}$
1	2.08×10^3	7.36×10^4
2	2.08×10^3	7.36×10^4
3	1.76×10^2	7.74×10^4
4	2.22×10^8	1.61×10^5
5	8.32×10^4	1.25×10^5
6	2.50×10^5	1.25×10^5
7	1.14×10^5	1.25×10^5
8	4.77×10^7	1.25×10^5

$$IV = 2.1 \times 10^{-4} \, MW_N^{0.82} \,, \tag{2.21}$$

where $\mathcal{I} = \{$B-DEG, B-EG, B-TPA$\}$, $\mathcal{J} = \{$T-DEG, T-EG, T-TPA, T-VIN$\}$, and MW is the molecular weight of component i (Table A.1).

2.3 Results and Discussion

The modelling setup is a reactor dynamic model for producing PET that is used to compare the start-up phase of the process with the results reported in Seavey and Liu (2009).

2.3.1 Computational Implementation

The kinetic model was implemented in the programming language GNU Octave. GNU Octave is a high level computational language used to solve linear and nonlinear problems numerically and performing other numerical experiments as well as process simulations. The solution of the ordinary-differential equations system was obtained with `lsode` (or Livermore Solver for Ordinary Differential Equations) solver (Hindmarsh, 2006). `lsode` is a part of ODE-PACK collection and obtains the solution for equations with the form $dy/dt = f(t, y)$.

Structurally, the implemented code is composed by a main program depending on two principal functions, which calls other small functions (Figure 2.2). These secondary func-

17

tions are grouped in two sets. One group is related to the calculations of components properties (identified by `_props_`), and the other one related to phase characteristics (identified by `_phase_`).

```
Main program
    └── fun_F.m
            └── fun_PETREACTION.m
                    ├── fun_props_GETDATA.m
                    ├── fun_props_LIMITMOLES.m
                    ├── fun_props_LIMITT.m
                    ├── fun_props_LMVCOMP.m
                    ├── fun_props_MIXLMV.m
                    ├── fun_props_MOLEFRAC.m
                    ├── fun_phase_CONCVOL.m
                    ├── fun_phase_MOLETOMASS.m
                    ├── fun_phase_SOLLIQFLUX.m
                    ├── fun_phase_SOLUBILITY.m
                    └── fun_phase_VOLUME.m
```
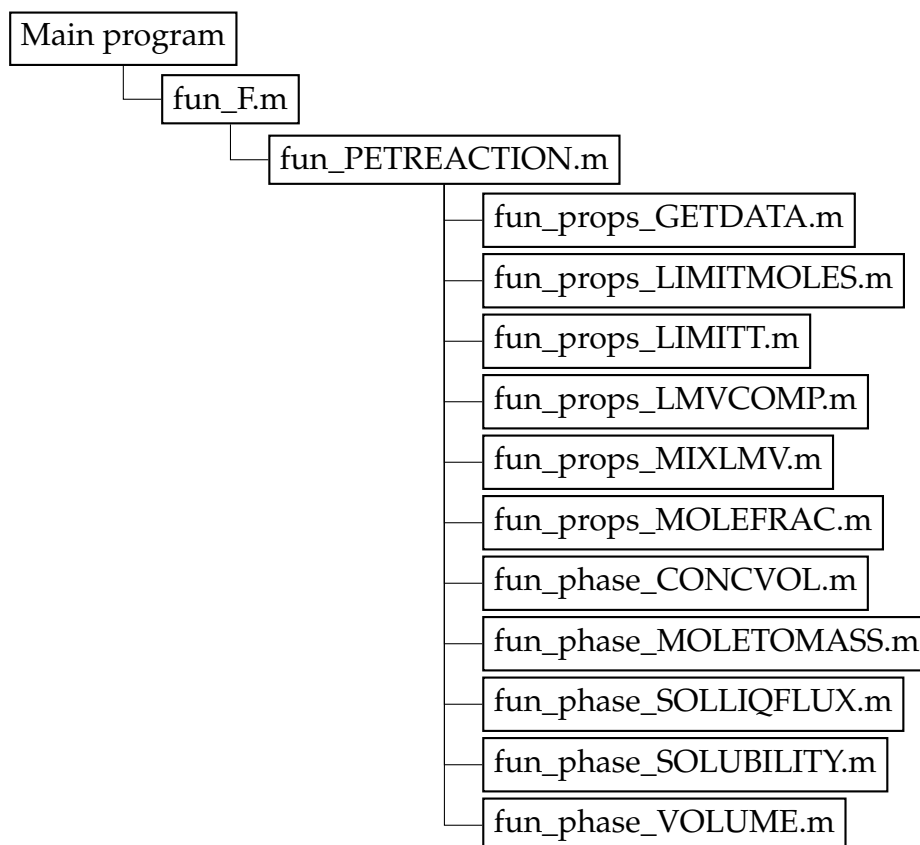
Figure 2.2: Function dependency flowchart used for the computational implementation of the batch reactor.

The main program is found in `design_batch_PET.m` function. Species balances derivatives are computed in `fun_F.m` function, and rate reactions are calculated in `fun_PETREACTION.m`. The properties and phase related functions are implemented in several files described in Figure 2.2.

- `fun_props_GETDATA.m` - get physical property values for each component: molecular weight (kg mol^{-1}), critical properties (critical temperature, K, pressure, Pa, and compressibility), vapour pressure (Pa), liquid density (kmol m^{-3}), vapour and liquid viscosity (Pa s).

- `fun_props_LIMITMOLES.m`, `fun_props_LIMITT.m` - limit the molar flowrate and temperature, respectively, between minimum and maximum values.

- `fun_props_LMVCOMP.m` - compute the pure-component liquid molar volume (mol^3 mol^{-1}). Segments of components are set to zero.

- `fun_props_MIXLMV.m` - calculate mixture liquid molar volume (m^3 mol^{-1}) using the Amagat's law.

- `fun_props_MOLEFRAC.m` - compute molar fractions.

- `fun_phase_CONCVOL.m` - compute the concentration of each component in liquid phase ($mol\ m^{-3}$).

- `fun_phase_MOLETOMASS.m` - compute mass flow ($kg\ s^{-1}$) concerted from molar flow ($mol\ s^{-1}$).

- `fun_phase_SOLLIQFLUX.m` - compute the mass-transfer flux from the solid to the liquid phases ($mol\ m^{-2}\ s^{-1}$).

- `fun_phase_SOLUBILITY.m` - calculate the solubility of each component in the liquid phase ($mol\ m^{-3}$).

- `fun_phase_VOLUME.m` - compute the volumetric flowrate ($m^3\ s^{-1}$) from the amount of molar flow ($mol\ s^{-1}$).

The computer program ran on a personal computer with an Intel Core i7 2.5GHz processor under the GNU Linux operating system.

2.3.2 Open-Loop Simulation

The results presented below were obtained for a time horizon of 180 min with a sampling time of 1 min. In this simulation study, liquid EG and solid TPA are initially charged to the batch reactor setting their mass ratio to 1.5 at atmospheric pressure. Reactor temperature is imposed with a profile changing between 200 and 250 °C, according to Figure 2.3.

For validation purposes, the simulated results are compared with the literature data obtained from Seavey and Liu (2009) for the same operating conditions. Figure 2.4 shows the molar holdups of each component in both liquid and solid phases identifying simulation data with sim and literature data with lit. In all the six plots of Figure 2.4, it is possible to observe that simulated data are in accordance with the literature results. All components achieve steady-state around 100 min, with the exception of AA that is present on the reaction in very small
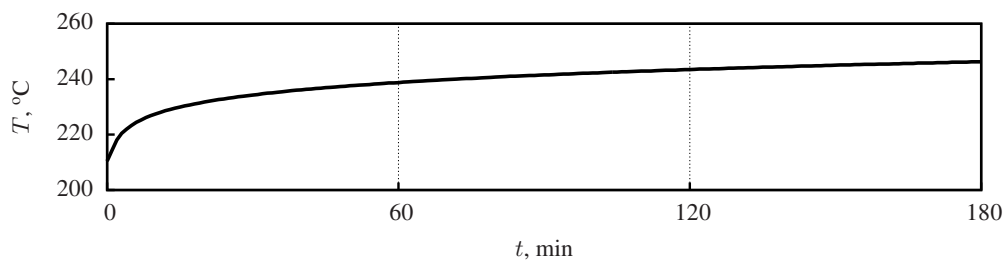
Figure 2.3: Batch esterifier temperature.
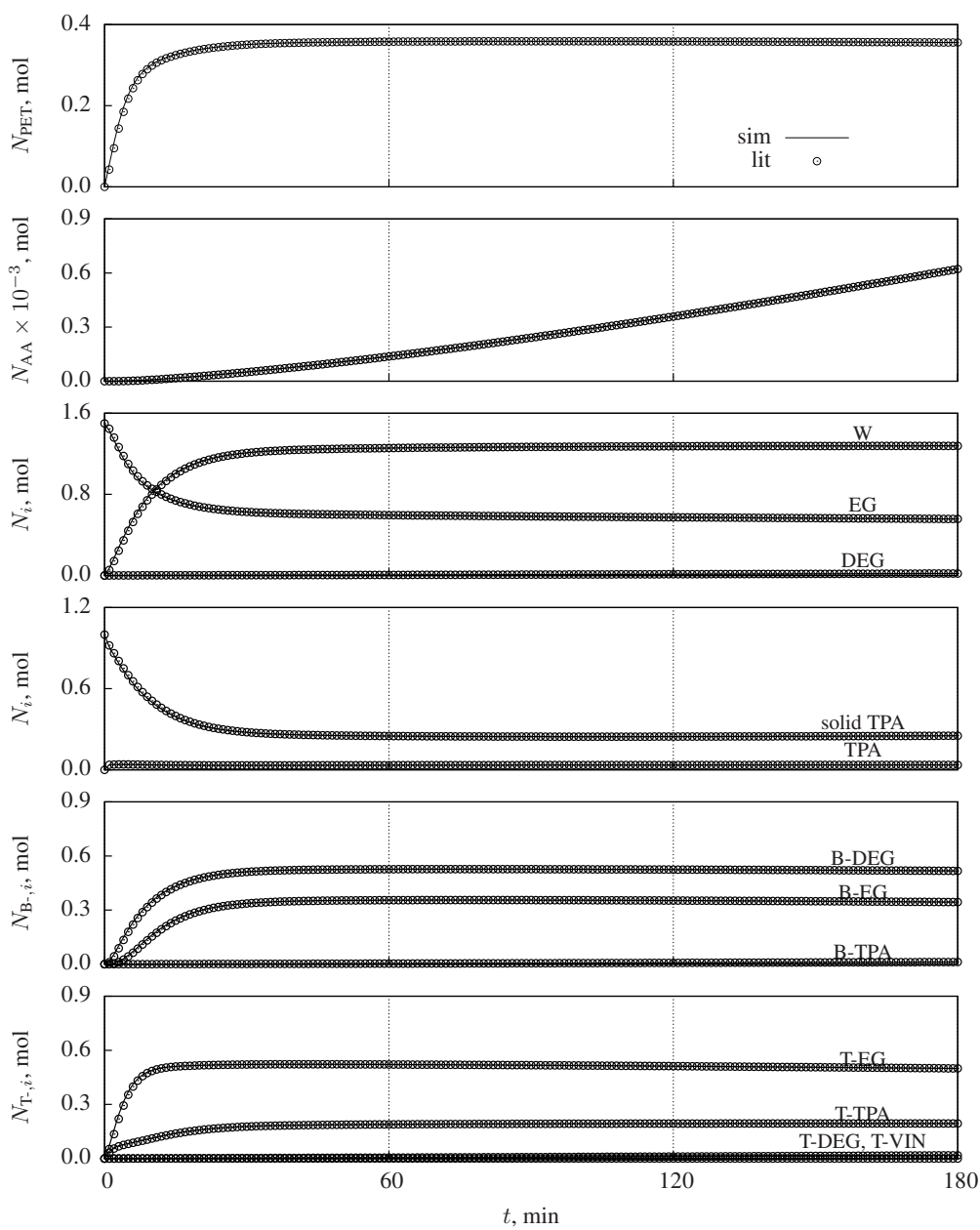
Figure 2.4: Molar holdups in batch esterifier liquid and solid phases.

quantities (around 1.2×10^{-3} mol as can be seen in the second plot of Figure 2.4). Its worth mention that this component is mainly produced in final stages of PET production process. At the end of the reaction, 74.78 % of the initial solid TPA is dissolved and 62.81 % of initial liquid EG is consumed reaching the 0.25 mol and 0.60 mol, respectively (see third and fourth plots of Figure 2.4). In these operational conditions, TPA is sharply the limiting reactant because, while it dissolves, it immediately reacts with EG (liquid TPA shows very low values in the fourth plot). PET reaches quantities of 0.34 mol after the steady-state being achieved .

Water is one of the products formed in larger amounts with values of 1.30 mol (third plot of Figure 2.4) followed up by the segments groups B-DEG and T-EG (see the fifth and sixth plots).

Some polymer properties, intrinsic viscosity and number-average molecular weight are depicted in Figure 2.5. At the end of the batch their values are 0.585 dL g^{-1} and 0.426 kg mol^{-1}, respectively.
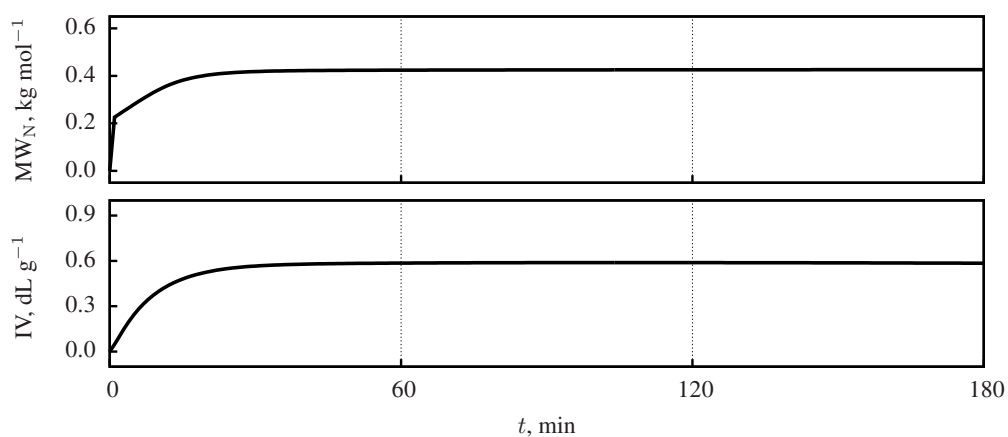
Figure 2.5: PET properties.

Chapter 3

Modelling of a Continuous Dynamic Esterifier

The present chapter describes the dynamic model of a continuous esterifier where PET polymer is produced. The implemented model was tested and the obtained simulation results are compared to those reported in the literature. In addition, a study of the process operating window is developed.

3.1 Mathematical Modelling

The esterifier consists of a continuous reactor fed with solid TPA and liquid EG. This reactor is modelled as an isothermal multi-phase stirred tank considering vapour, liquid, and solid phases. The main model assumptions are (Seavey and Liu, 2009):

- reaction only occurs in the liquid phase;

- all the phases are treated individually;

- solid and liquid phases only interact by mass-transfer due to dissolution;

- mass-transfer between liquid and vapour occurs by diffusion;

- the temperature of all the three phases is the same;

- feed flowrate is composed by solid phase dispersed in liquid;

- the condensate flow total volume includes solid and liquid contributions;

- the amount of solid is always proportional to the volume.

The multi-compartmental model considers the simplified scheme presented in Figure 3.1. Two streams enter the reactor: a liquid stream with flowrate $F_{\text{liq}}^{\text{in}}$ and composition $x_{\text{in},i}$, and a solid stream with flowrate $F_{\text{sol}}^{\text{in}}$ and composition $z_{\text{in},i}$. The three phases are characterised by molar holdup, $N_{j,i}$, and volume V_j (where j represents the phase and assume values of $j \in \{\text{vap}, \text{liq}, \text{sol}\}$ and i represents the components). Vapour, liquid, and solid phases are also characterised by their molar fractions of each component i, y_i, x_i, and z_i, respectively. All phases are interconnected exchanging mass between them. From each phase a stream leaves with the phase composition and flowrate F_j^{out}.
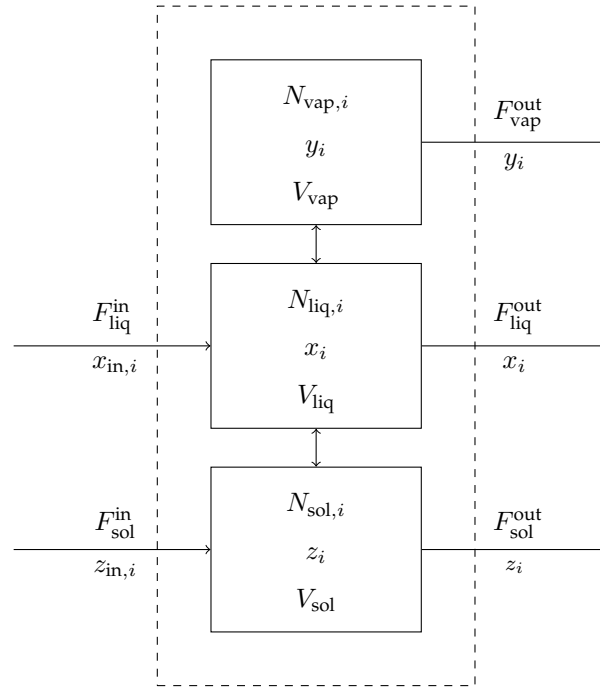
Figure 3.1: Multi-compartmental model scheme.

The global molar balance for each phase is described by

$$\frac{\mathrm{d}N_{\text{sol},i}}{\mathrm{d}t} = F_{\text{sol}}^{\text{in}}\, z_{\text{in},i} - F_{\text{sol}}^{\text{out}}\, z_i - n_{\text{sol-liq},i}\, A_{\text{sol-liq}}\,, \tag{3.1}$$

$$\frac{\mathrm{d}N_{\text{liq},i}}{\mathrm{d}t} = F_{\text{liq}}^{\text{in}}\, x_{\text{in},i} - F_{\text{liq}}^{\text{out}}\, x_i - n_{\text{liq-vap},i}\, A_{\text{liq-vap}} + n_{\text{sol-liq},i}\, A_{\text{sol-liq}} + r_j V_{\text{liq}}\,, \tag{3.2}$$

$$\frac{\mathrm{d}N_{\text{vap},i}}{\mathrm{d}t} = F_{\text{vap}}^{\text{in}}\, y_{\text{in},i} - F_{\text{vap}}^{\text{out}}\, y_i - n_{\text{liq-vap},i}\, A_{\text{liq-vap}}\,, \tag{3.3}$$

where r_j is the reaction rate for reaction j defined in Chapter 2 (page 13), $A_{\text{sol-liq}}$ and $A_{\text{liq-vap}}$ are solid-liquid and liquid-vapour interfacial areas (m^2), respectively, and $n_{\text{sol-liq},i}$ and $n_{\text{liq-vap},i}$ are the mass-transfer flux due to the dissolution between solid and liquid and diffusion between

liquid and vapour (mol m^{-2} s^{-1}), respectively.

To evaluate the polymerisation evolution, some quality parameters should be monitored. Besides the intrinsic viscosity and the number-average molecular weight (calculated by (2.20) and (2.21)), reaction conversion also gives valuable indication of reaction evolution for the chosen conditions. Here, reaction conversion, χ (%(m/m)), is mathematically defined using

$$\chi = \frac{F_{\text{liq}}^{\text{out}} \, x_{\text{PET}} \, \text{MW}_{\text{N}}}{\dot{m}_{\text{in}}} \, 10^2 \,. \tag{3.4}$$

where $\dot{m}_{\text{in}}$ is the liquid and solid mass flowrates, in kg s^{-1}, respectively.

Output Flowrates

Considering that both liquid and solid phases contribute to the total tank volume, output liquid-solid flowrate is calculated based on the fact that the liquid phase volume is a proportionate amount of the solid one, V_{sol}. Using a controller to maintain the total volume constant, $V_{\text{liq}} + V_{\text{sol}}$, the output flowrates are mathematically described as (Seavey and Liu, 2009)

$$F_{\text{sol}}^{\text{out}} = \begin{cases} 0 & , \text{ if } V_{\text{liq}} + V_{\text{sol}} \leq V_{\text{sp}} \\ \frac{V_{\text{sol}}}{V_{\text{liq}}+V_{\text{sol}}} \, \varphi_{\text{liq}-\text{sol}} \, (V_{\text{liq}} + V_{\text{sol}} - V_{\text{sp}})^{\frac{3}{2}} & , \text{ if } V_{\text{liq}} + V_{\text{sol}} > V_{\text{sp}} \end{cases}, \tag{3.5}$$

and

$$F_{\text{liq}}^{\text{out}} = \begin{cases} 0 & , \text{if } V_{\text{liq}} + V_{\text{sol}} \leq V_{\text{sp}} \\ \left(1 - \frac{V_{\text{sol}}}{V_{\text{liq}}+V_{\text{sol}}}\right) \varphi_{\text{liq}-\text{sol}} \, (V_{\text{liq}} + V_{\text{sol}} - V_{\text{sp}})^{\frac{3}{2}} & , \text{if } V_{\text{liq}} + V_{\text{sol}} > V_{\text{sp}} \end{cases}, \tag{3.6}$$

where V_{sp} is the reactor total volume setpoint (m^3) and $\varphi_{\text{liq}-\text{sol}}$ the weir constant (mol s^{-1} m$^{-\frac{9}{2}}$).

The output vapour flowrate is calculated based on the flowrate through a valve using

$$F_{\text{vap}}^{\text{out}} = \begin{cases} 0 & , \text{if } P \leq P_{\text{SP}} \\ \varphi_{\text{vap}} \, (P - P_{\text{SP}})^{0.5} & , \text{if } P > P_{\text{SP}} \end{cases}, \tag{3.7}$$

where φ_{vap} is the vapour phase flow constant in mol s^{-1} Pa$^{-0.5}$. Pressure is defined by the ideal

gas law written as

$$P = \frac{\left(\sum_i N_{\mathrm{vap},i}\right) R\,T}{V_{\mathrm{vap}}}\,, \tag{3.8}$$

where V_{vap} is the vapour phase volume (m^3).

Mass-transfer limited rates

Neglecting the mass transfer resistance in the vapour phase, the diffusion term between vapour and liquid is quantified by penetration theory through (mol m^{-2} s^{-1}) (Seavey and Liu, 2009)

$$n_{\mathrm{liq-vap},i} = \sqrt{\frac{D_i}{\pi\,t_{\mathrm{c}}}} \left(\frac{y_i\,P}{\nu_i\,\gamma_i\,P_i^{\mathrm{sat}}} - C_{\mathrm{liq},i}\right), \quad \forall i \in \mathcal{U} = \{\mathrm{AA, DEG, EG, W}\}, \tag{3.9}$$

where D_i is the molecular diffusivity (m^2 s^{-1}), t_{c} is the number-average contact time between a given parcel of liquid and vapour (s), ν_i is the pure-component molar volume (m^3 mol^{-1}), γ_i is the activity coefficient (dimensionless), and P_i^{sat} is the vapour pressure of pure species i (Pa). For components that do not belong to $\mathcal{U}$, $n_{\mathrm{liq-vap},i}$ is set to zero.

Because solid particles are composed by 100 % of TPA, the dissolution rate of solid into liquid occurs only for TPA being computed using

$$n_{\mathrm{sol-liq,TPA}} = k_{\mathrm{s}}\left(\alpha - C_{\mathrm{liq,TPA}}\right). \tag{3.10}$$

For all the other components, $n_{\mathrm{sol-liq},i}$ is considered as zero.

Vapour Pressure

Modified Antoine Equation is used to calculate pure component vapour pressure by

$$P_i^{\mathrm{sat}} = \exp\left(A_i + \frac{B_i}{T} + C_i \ln T + D_i\,T^{E_i}\right) \tag{3.11}$$

where A_i, B_i, C_i, D_i and E_i are constants valid in the range of $F_i \leq T \leq G_i$. These parameters are expressed in Table A.2 of Appendix A. Since vapour pressure parameters are not well known for solid TPA and BHET, they are considered as non-volatile species, thus, A_i is set to -40 and all the other parameters are set to zero (Seavey and Liu, 2009).

Liquid-Vapour Equilibrium

Although the vapour mixture is considered ideal, polymers mixtures are non-ideal and do not allow the application of the Raoult's Law. Consequently, the liquid-vapour equilibrium is defined by

$$P_i = x_i \, \gamma_i(x_i, T) \, P_i^{\text{sat}}(T) \,, \tag{3.12}$$

where P_i is the component pressure (Pa), in order to calculate the vapour pressure, $P = \sum_i P_i$.

The activity coefficient is calculated based on the polyNRTL model by (Chen, 1993)

$$\ln \gamma_i = \ln \gamma_i^{\text{NRTL}} + \ln \gamma_i^{\text{FH}} \,, \tag{3.13}$$

where γ_i^{NRTL} and γ_i^{FH} are the non-random two-liquid (NRTL) and the Flory-Huggins (FH) contributions, respectively, to the activity coefficient of species i.

Flory-Huggins contribution is written as

$$\ln \gamma_i^{\text{FH}} = \ln \frac{\phi_i}{x_i} + 1 - d_i \sum_j \frac{\phi_j}{d_j} \,, \tag{3.14}$$

where d_i is the degree of polymerisation obtained by

$$d_i = \frac{\text{MW}_{\text{N}}}{\text{MW}_{\text{PET monomer}}} \,, \tag{3.15}$$

$\text{MW}_{\text{PET monomer}}$ is the PET repeating unit molecular weight, and ϕ_i is calculated based on the segment-based mole fraction, X_i, using the criteria

$$\phi_i = \begin{cases} 0 & , \text{for } i = \text{PET} \\ \\ X_i & , \text{otherwise} \end{cases} \,, \tag{3.16}$$

with

$$X_i = \frac{x_i}{\displaystyle\sum_j^{\text{All species}\backslash\text{PET}} x_j} \,. \tag{3.17}$$

The polyNRTL contribution for a solvent s is obtained by

$$\ln \gamma_{\text{s}}^{\text{NRTL}} = \frac{\sum\limits_{k} X_k\, G_{k,\text{s}}\, \tau_{k,\text{s}}}{\sum\limits_{k} X_k\, G_{k,\text{s}}} + \sum\limits_{l} \frac{X_l\, G_{\text{s},l}}{\sum\limits_{k} X_k\, G_{k,l}} \left(\tau_{l,\text{s}} - \frac{\sum\limits_{k} X_k\, G_{k,l}\, \tau_{k,l}}{\sum\limits_{k} X_k\, G_{k,l}} \right), \tag{3.18}$$

and for the polymer p by

$$\ln \gamma_{\text{p}}^{\text{NRTL}} = \sum\limits_{j} r_{\text{p},j} \left[\frac{\sum\limits_{k} X_k\, G_{k,j}\, \tau_{k,j}}{\sum\limits_{k} X_k\, G_{k,j}} + \sum\limits_{k} \frac{X_k\, G_{j,k}}{\sum\limits_{l} X_l\, G_{l,k}} \left(\tau_{j,k} - \frac{\sum\limits_{l} X_l\, G_{l,k}\, \tau_{l,k}}{\sum\limits_{l} X_l\, G_{l,k}} \right) \right], \tag{3.19}$$

with

$$G_{i,j} = \exp(-\varsigma\, \tau_{i,j}), \tag{3.20}$$

where $G_{i,j}$ represents the interaction between species i and j, ς is a randomness factor (usually set to 0.3), and $\tau_{i,j}$ is a binary interactions parameter defined by

$$\tau_{i,j} = A_{i,j} + \frac{B_{i,j}}{T} + C_{i,j}\ln T + D_{i,j}\, T, \tag{3.21}$$

$A_{i,j}$, $B_{i,j}$, $C_{i,j}$ and $D_{i,j}$ are constants presented in Table A.4 of Appendix A.

3.2 Smoothing of Discontinuous Models

Since the model is characterised by discontinuous nonlinear equations, mixed integer nonlinear optimisation tools are typically called for in the context of simulation and optimisation. However, the timing requirements of real-time optimisation and advanced process control usually preclude the use MINLP tools and, therefore, such models need to be transformed to become solvable with continuous optimisation tools. For instance, some approaches based on discontinuities smoothing may be applied to these equations. In the present work, two techniques were used in order to avoid discontinuities. The first approach considers the discontinuous system (Balakrishna and Biegler, 1992)

$$f(t) = \begin{cases} 0, & g(t) \le 0 \\ \\ g(t), & g(t) > 0 \end{cases}, \tag{3.22}$$

where $f(t)$ is a continuously differentiable real function. Function (3.22) is approximated by a smoothing function, $\widetilde{f}(t)$, with the form

$$\widetilde{f}(t) = \frac{\sqrt{g(t)^2 + \xi^2}}{2} + \frac{g(t)}{2} \, , \tag{3.23}$$

where ξ is an accuracy constant. This approach is quite simple and efficient, but when the function branches number increases the discontinuity problem may not be resolved. So, the smoothing of functions can be completed using the hyperbolic tangent (Abbo and Sloan, 1995; Kayihan and Doyle III, 2000; Sloan and Booker, 1986). Considering the general discontinuous system

$$f(t) = \begin{cases} f_1(t), & \text{if } t \in T_1 \\[2mm] f_2(t), & \text{if } t \in T_2 \\[2mm] \vdots \\[2mm] f_m(t), & \text{if } t \in T_m \end{cases} \, , \tag{3.24}$$

where $f_i(t)$, $i = 1, \cdots, m$, are continuously differentiable real functions subject to the conditions that define the subsets T_i defined as

$$T_i = \{t \in \mathbb{R}^n : e_k(t) < 0, \forall k \in L_i; e_k(t) \geq 0, \forall k \in G_i\} \, , \tag{3.25}$$

where L_i and G_i are, for branch i, the sets of indexes k for which $e_k(t) < 0$ and $e_k(t) \geq 0$, respectively. Expressions $e_k(t)$, with $k = 1, \cdots, p$, are continuously differentiable. Function (3.24) can be expressed using the Heaviside function, $\mathcal{H}$, as (Brásio et al., 2014)

$$f(t) = \sum_{i=1}^{m} \prod_{k \in L_i} [1 - \mathcal{H}(e_k)] \prod_{k \in G_i} \mathcal{H}(e_k) \, f_i(t) \, , \tag{3.26}$$

with

$$\mathcal{H}(e_k) = \begin{cases} 1, & \text{if } e_k \geq 0 \\[2mm] 0, & \text{if } e_k < 0 \end{cases} \, . \tag{3.27}$$

Now, the Heaviside function is approximated by

$$\widetilde{\mathcal{H}}(t) = 0.5 + 0.5 \cdot \tanh\left(\xi \cdot t\right) \, , \tag{3.28}$$

where $\widetilde{\mathcal{H}}(t)$ is the smoothed Heaviside function.

Therefore, (3.24) can be rewritten as

$$\widetilde{f}(t) = \sum_{i=1}^{m} \prod_{k \in L_i} \left[1 - \widetilde{\mathcal{H}}(e_k)\right] \prod_{k \in G_i} \widetilde{\mathcal{H}}(e_k) \, f_i(t) \,. \tag{3.29}$$

3.3   Results and Discussion

The simulations performed in this section consider reactor operating conditions at 10 atm, to prevent EG evaporation, and all the phases are at the same temperature of 260 ^{o}C, in order to promote the TPA solubility. The total flowrate of the inlet stream is 1.2626 kg s^{-1}. Additionally, the initial holdups inside the esterifier are: 10 mol of gaseous EG, 36.6×10^3 mol of liquid EG, and 13.7×10^3 mol of solid TPA. Liquid and solid holdups correspond to a mass ratio between liquid EG and total feed of 0.5. Simulations runs for 400 min with a sampling time of 1 min.

3.3.1   Computational Implementation

The dynamic model, implemented in GNU Octave, consists of a main program depending on other functions (Figure 3.2).

The purpose of the main program is to simulate the continuous esterifier reactor using LSODE solver. Function `fun_F.m` has the objective of computing the species balances. The reaction rates are given in `fun_PETREACTION.m`. Other auxiliary functions are described below.

- `fun_stirredtank_CONDENSEDFLOW.m` - computes the condensed flowrates (solid and liquid). In this case, the proportion of liquid and solid is considered to be equal.

- `fun_stirredtank_VAPORFLOW.m` - calculates the product vapour flowrates for each component (mol s^{-1}).

- `fun_props_MWN.m` - computes the molecular weight (kg mol^{-1}) of the polymer sample. This calculation is made based on segments moles and MW$_N$ (kg mol^{-1}).

- `fun_props_VAPORPRESSURE.m` - calculates pressure (Pa). For segments is set to 1×10^{-40} Pa.

- `fun_phase_GETBINARIES.m` - gets the binaries interaction parameters.
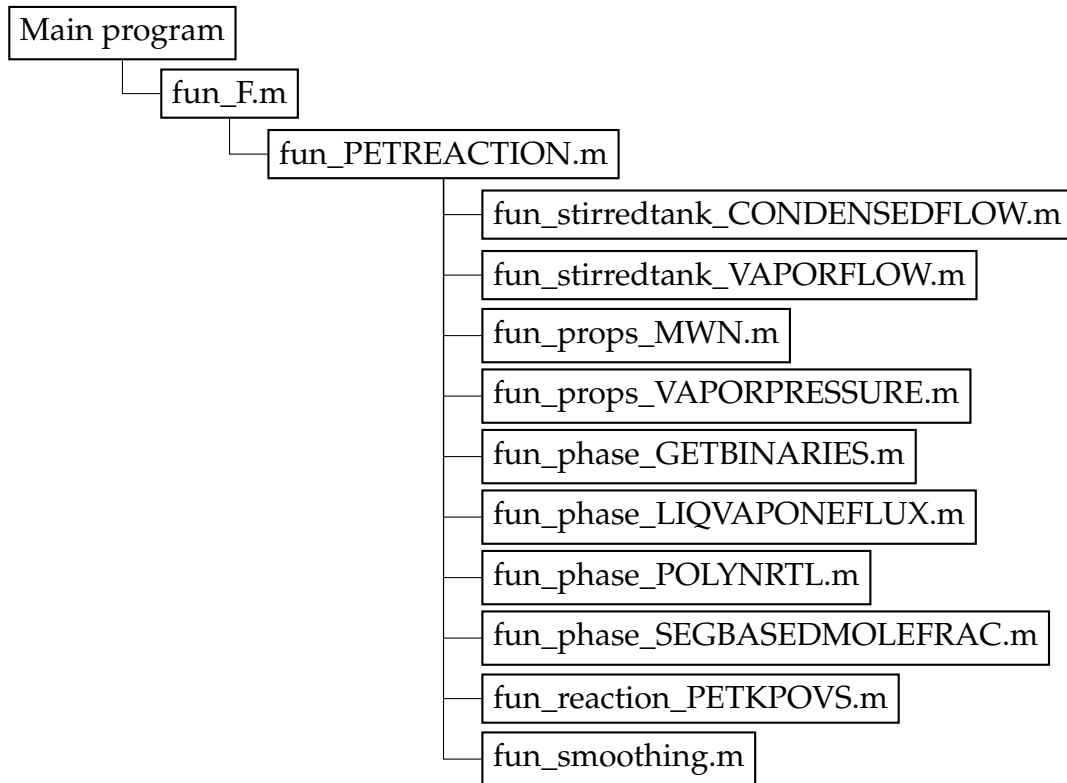
Figure 3.2: Function dependency flowchart used for the computational implementation of the continuous reactor.

- `fun_phase_LIQVAPONEFLUX.m` - computes the mass transfer flux of vapour-liquid considering only the liquid side mass transfer resistance.

- `fun_phase_POLYNRTL.m` - computes the activity coefficient.

- `fun_phase_SEGBASEDMOLEFRAC.m` - computes the segment-based mole fraction for a liquid mixture (n/n).

- `fun_reaction_PETKPOVS.m` - computes the intrinsic viscosity (dL g^{-1}).

- `fun_smoothing.m` - computes function smoothing.

The functions implemented in the kinetics description in Chapter 2 are also necessary. Appendix C contains an example of the implemented source code of the simulator. The computer program ran on a personal computer with an Intel Core i7 2.5 GHz processor under the GNU Linux operating system.

3.3.2 Reactor Start-Up

This study assumes that the esterifier operates at a temperature of $T = 260\,^{\circ}\text{C}$ and a mass ratio between liquid feed EG and total feed $R_{\text{EG}} = 0.5$. The Simulation (sim) and literature (lit) results are draw in Figures 3.3 to 3.5 the literature data of Seavey and Liu (2009), that was also used in the comparison performed in Section 2.3.2. The reactants, PET and main side products (AA, W, and DEG) molar holdups are shown in Figure 3.3, the molar holdups of the components present in the vapour phase are present in Figure 3.4, and the segments molar holdups are depicted in Figure 3.5.

It is noteworthy that the simulation results reproduce well the literature data. Small differences appear near the 45 and 90 min time marks, especially visible in the fifth plot of Figure 3.3 and in the first plot of Figure 3.5. These discrepancies are the reflection of the model discontinuity smoothing necessary for the application of common non-integer optimisation tools.

Since the system simulation was not started at the steady-state, the profiles reveal a distinctive behaviour in the initial period stabilising around the 300 min. Solid TPA holdup drastically reduces in the first sampling time mainly due to the fast solid-liquid equilibrium and, then, increases smoothly until the steady-state (second plot of Figure 3.3). At the same time, liquid EG holdup decreases as it is almost all consumed by the reaction or transferred to the vapour phase. The liquid EG is not completely consumed, because the reactional system is composed by equilibrium reactions (first plot of Figure 3.3).

The side products DEG, AA and W are also produced in the reaction (fifth and sixth plots of Figure 3.3). Meanwhile, they are separated to the vapour by mass-transfer (Figure 3.4). DEG is the most transferred component to the vapour phase, in liquid phase reaches values near to zero. DEG is a key component for the product quality, as final PET properties are greatly dependent on the amount of this component that is mostly incorporated in PET polymer in the earlier stages. Although AA is produced in very low quantities by the reaction, these amounts must be carefully monitored because it is a quality control parameter in industries, specially when the produced PET is applied in bottles of water (Processing, 2009).

Some quality variables are also plotted to complement the previous results. Simulated reaction conversion, number-average molecular weight, and intrinsic viscosity are depicted in Figure 3.6. Reaction conversion increases according to the output liquid flowrate of PET drawn in Figure 3.7 reaching values of 23.82 %. This flowrate is manipulated to control the reactor volume as shown by (3.5),(3.6) and (3.7). In an initial phase, while the dynamic model of the
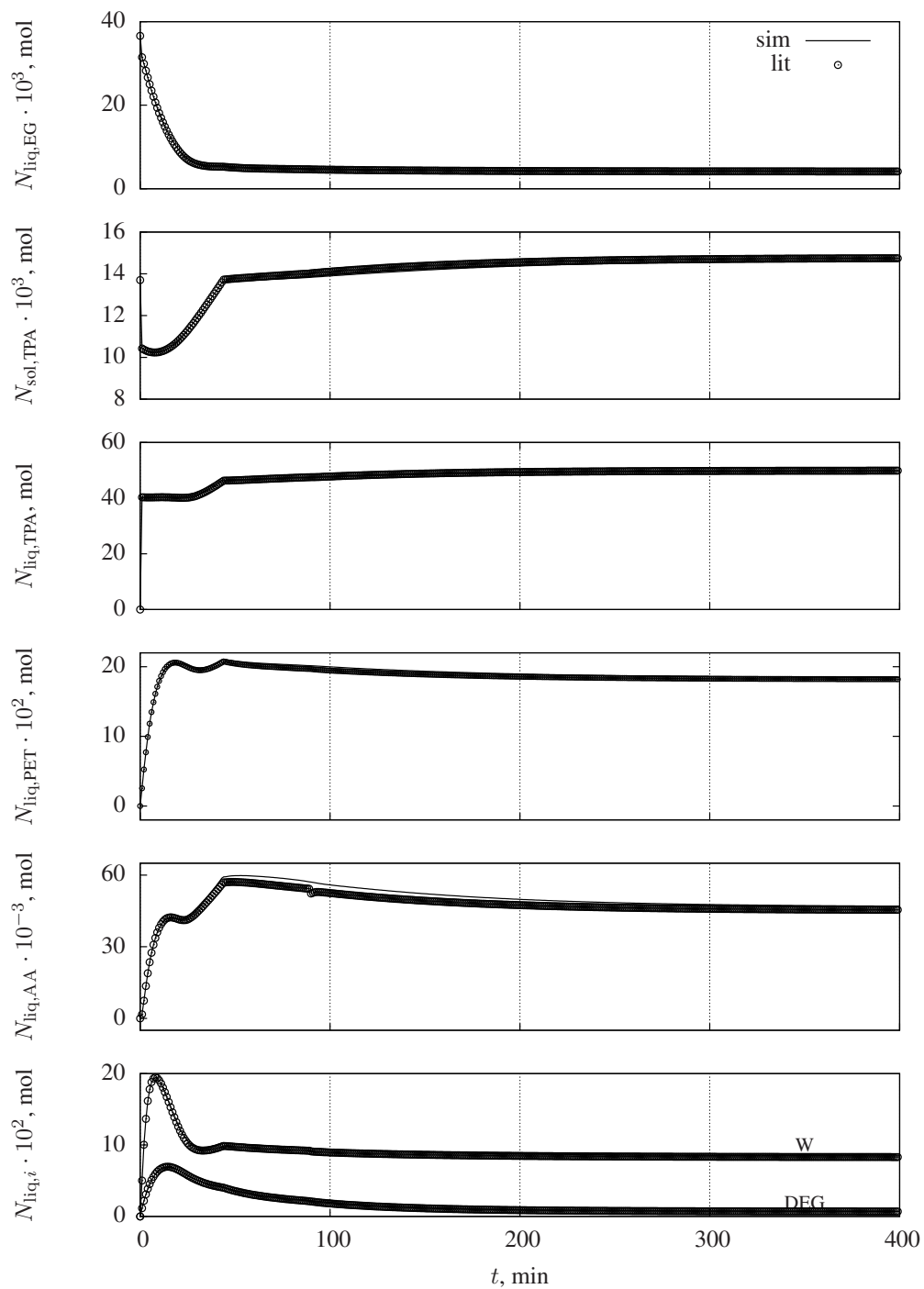
Figure 3.3: Molar holdups in the continuous esterifier liquid and solid phases.

continuous reactor does not reach the steady-state, the total output flowrate is zero to avoid that the reactor volume drops below the setpoint. Then, it is increased reaching quickly the steady-state. Intrinsic viscosity and number-average molecular weight smoothly increase along the time reaction obtaining values of $0.048\,\mathrm{dL\ g^{-1}}$ and $0.758\,\mathrm{kg\ mol^{-1}}$, respectively.

All components mass fractions can be observed in Figure 3.8 as well as the zoom in to DEG
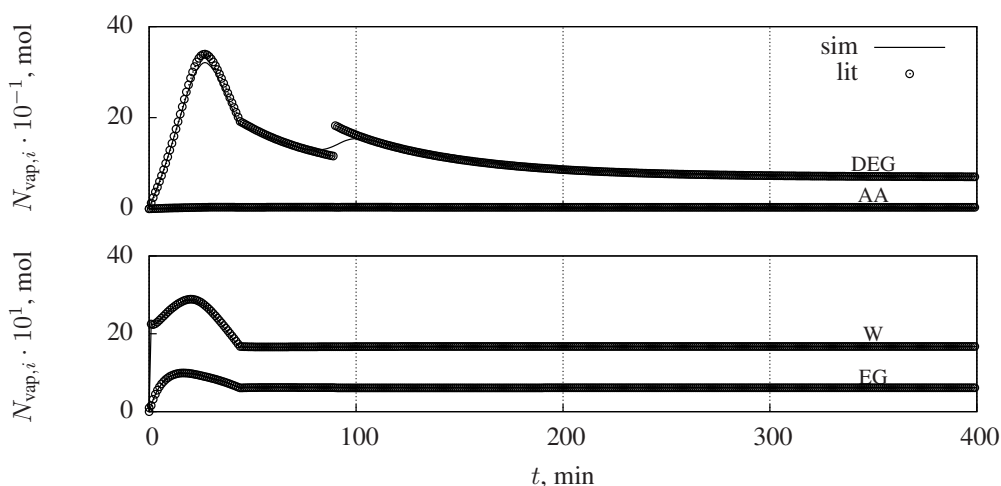
Figure 3.4: Molar holdups in the continuous esterifier vapour phase.
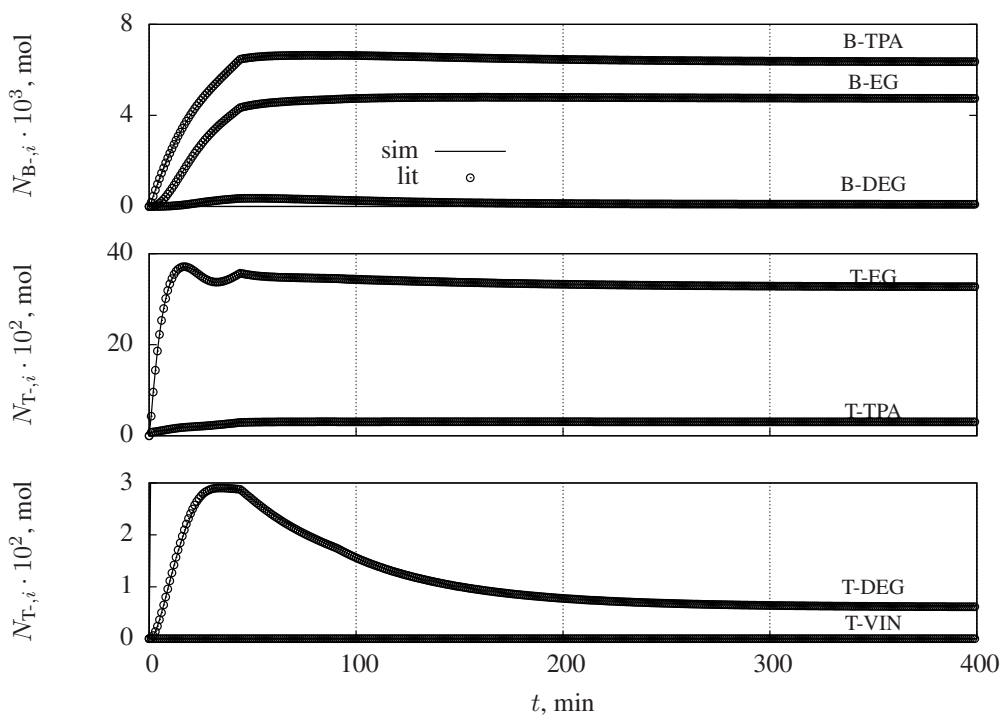
Figure 3.5: Segment molar holdups in the continuous esterifier liquid phase.

mass fraction profile and a zoom in the final compositions of components present in small quantities. At steady-state, the predominant component in the liquid phase is PET with a composition of 54.67 %(m/m) followed by EG with a value of 40.50 %(m/m). The percentage of DEG in liquid mixture is equal to 1.20 %(m/m).
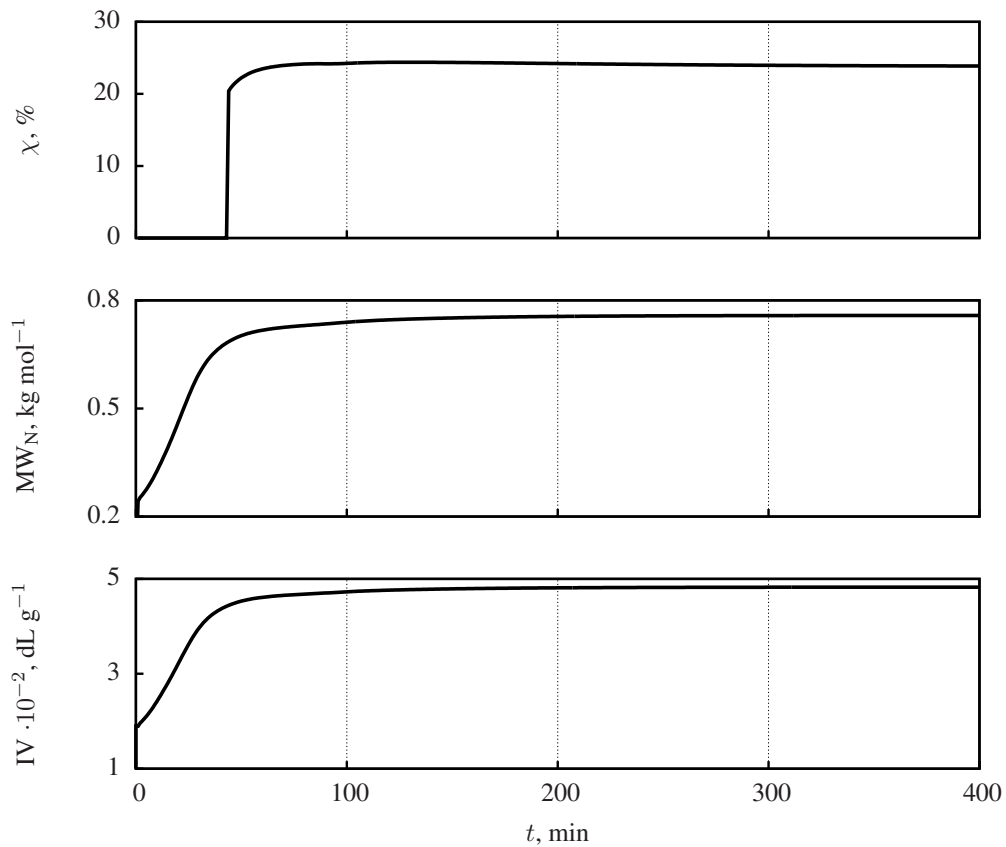
Figure 3.6: Polymer properties.
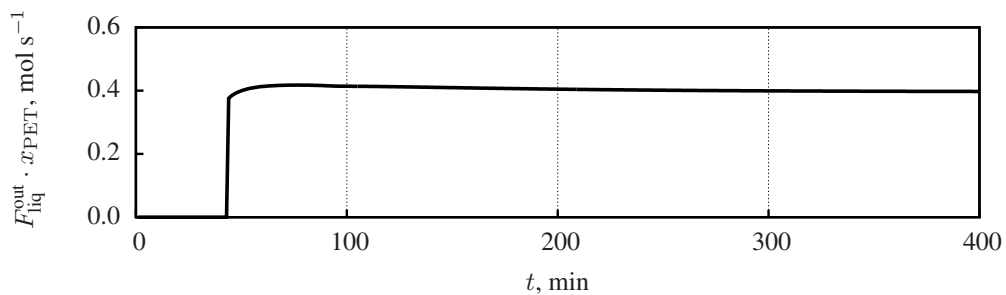
Figure 3.7: Output liquid flowrate of PET.

3.3.3 Operation Window Study

The mass ratio R_{EG} and the temperature T are key process parameters which means that higher reaction conversions and production rates may be attained using optimised values of these parameters. In this section, their influence on the process is studied while holding the remaining operating conditions constant.

This process is at steady-state point of $t = 400\,\mathrm{min}$. Process parameters R_{EG} and T are
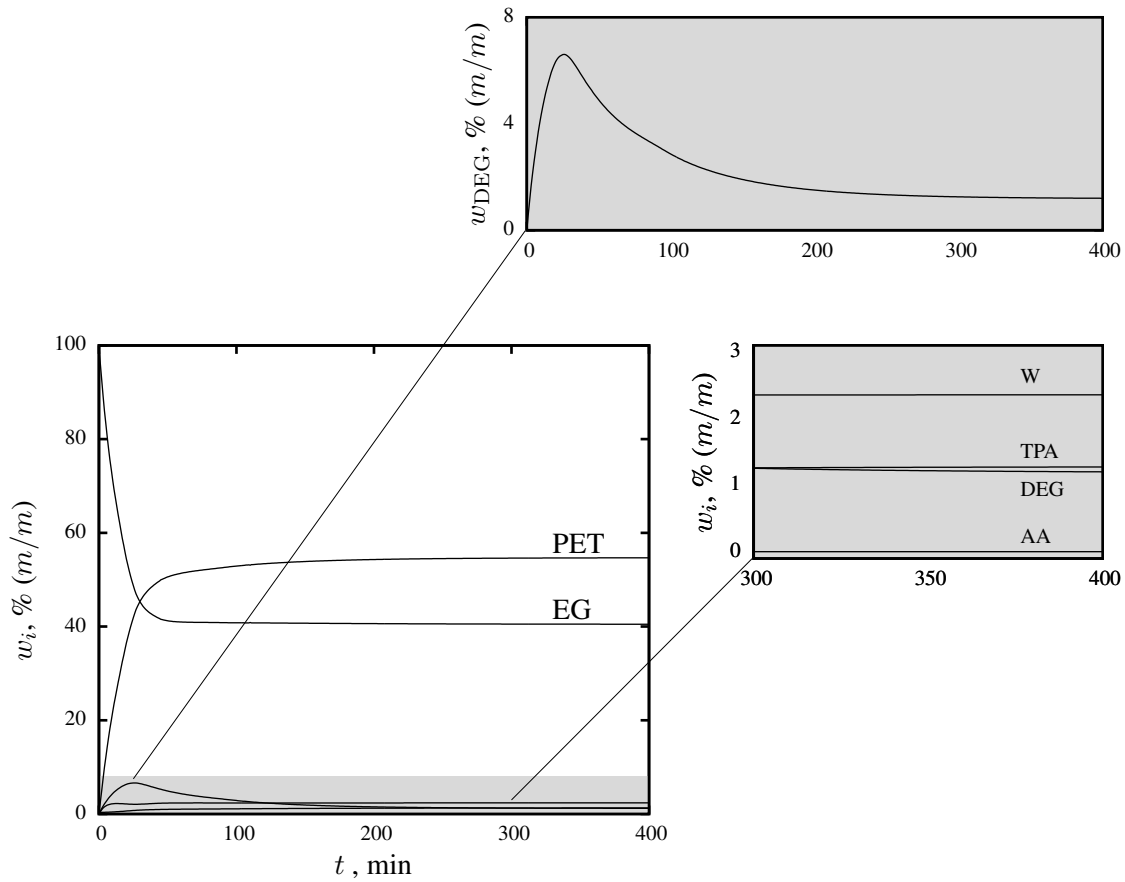
Figure 3.8: Component mass fraction in the reactor.

changed according to

$$0.1 < R_{EG} < 0.9, \qquad \Delta R_{EG} = 0.05,$$

$$246^{o}C < T < 286^{o}C, \qquad \Delta T = 2^{o}C.$$

The 3D profiles for the reaction conversion, the intrinsic viscosity, the PET production rate, and the number-average molecular weight are depicted in Figure 3.9. The evolution of the four process variables is quite irregular. For instance, Figures 3.9b and 3.9d shows that IV and MW_N increase with the increasing of ratio and temperature. In contrast, reaction conversion and PET production in Figures 3.9a and 3.9c do not present the same behaviour. For each T, there is a specific ratio R_{EG} in which the maximum conversion or production is achieved.

To illustrate this, 2D profiles were draw fixing a specific process variable ($R_{EG} = 0.5$ or $T = 260\,^{o}C$). Figures 3.10 and 3.11 show these profiles.

The results observed in first plot of Figure 3.10 indicate that the conversion increases when
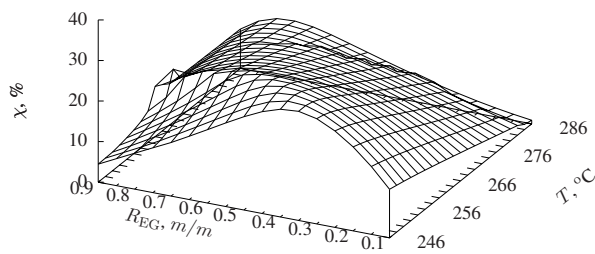
(a) Reaction conversion.
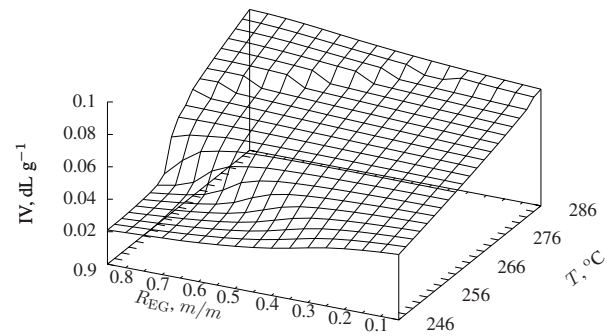
(b) Intrinsic viscosity.
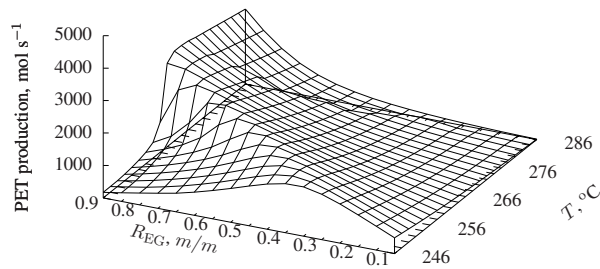
(c) PET production rate.
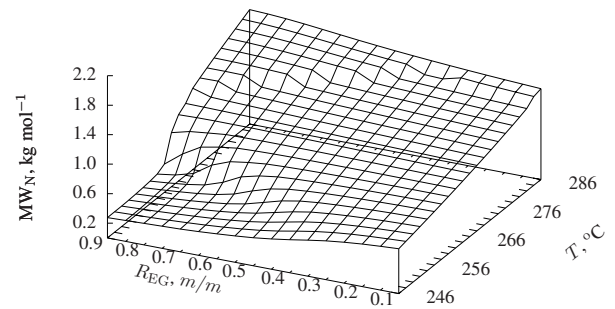
(d) Number-average molecular weight.

Figure 3.9: Effect of ratio R_{EG} and temperature on key operating variables.
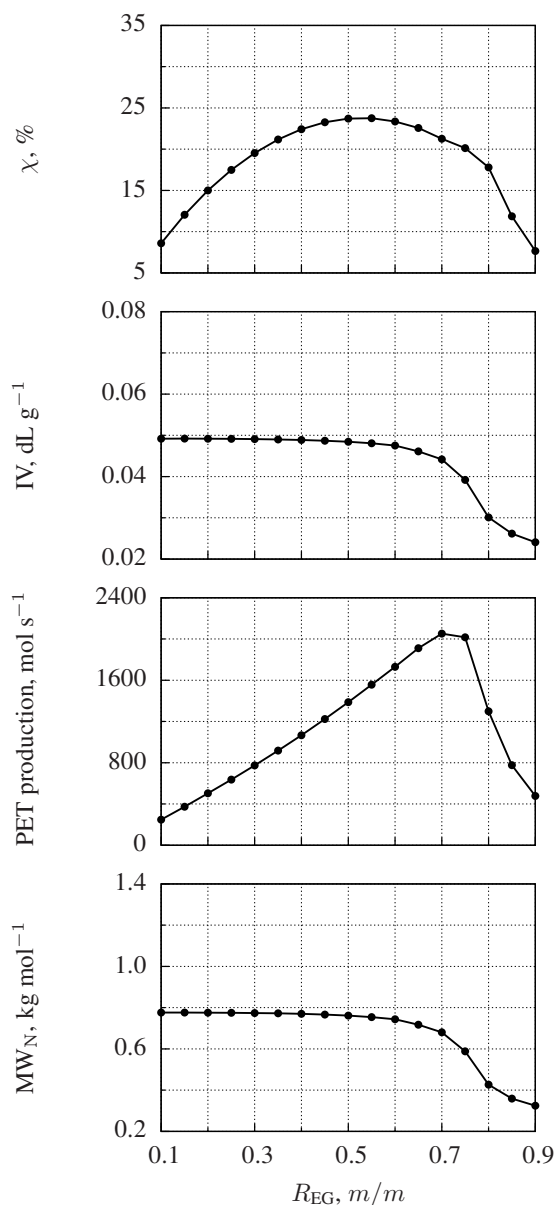
Figure 3.10: Effect of ratio R_{EG} ($T = 260$ºC).
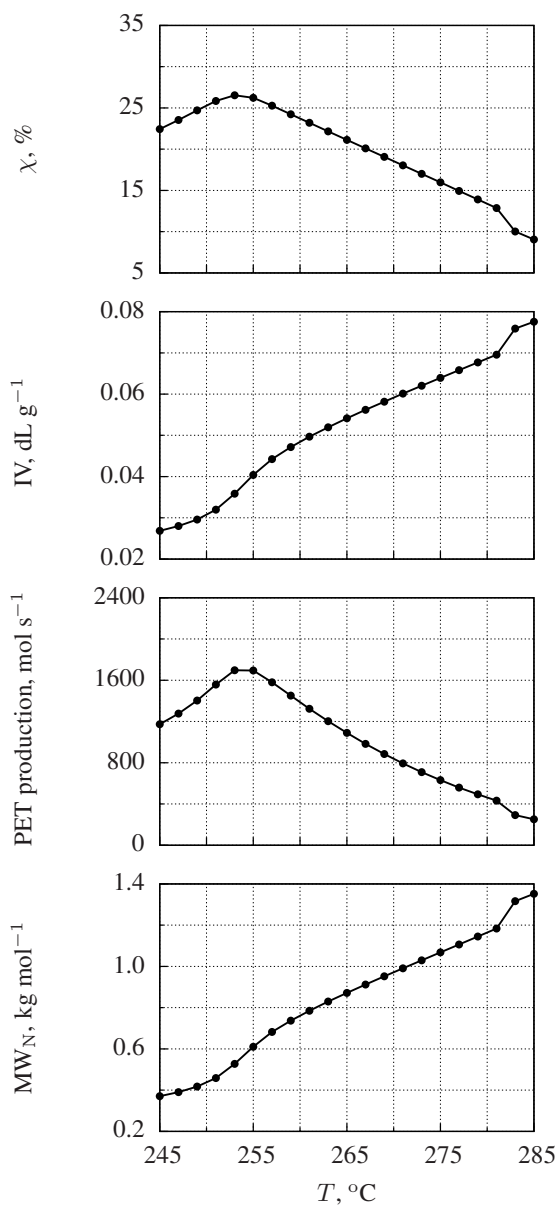
Figure 3.11: Effect of temperature ($R_{EG} = 0.5$).

more EG is available in the reaction. This occurs because it enlarges the amount of solid TPA soluble in the solvent. However, the use of more EG is not economical as it requires larger energy use for its vaporisation and condensation. The Temperature is another process variable that greatly influences the solubility of the solid TPA (TPA solubility is augmented with the temperature increasing). By contrast, the increase of liquid may promote forward reaction of the esterification. Kang et al. (1996) also refers that excess of liquid TPA can act as an acidic catalyst for the reactions reducing conversion. These aspects justify the profile observed in Figure 3.9a where maximum conversions are found in the ranges of 0.4 to 0.6 (m/m) and 250

to 260 °C. Figure 3.9a also presents an abrupt behaviour occurring for R_{EG} in the range of 0.8 to 0.9 and temperatures around the 260 °C. Figure 3.12 zooms in these ranges with smaller increments on R_{EG} and T allowing to verify that the peak smoothed out.
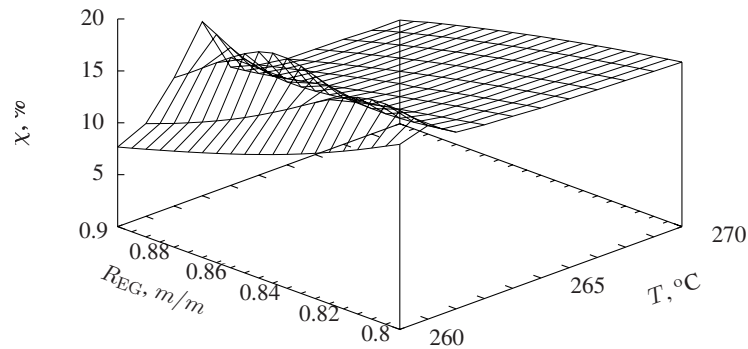
Figure 3.12: PET conversion zoom in for ratios of 0.8 to 0.9 (m/m) and for temperatures of 260 to 270 °C.

The increasing of the ratio between feed EG and total feed (more introduction of EG) induces more PET production when the temperature of reaction is set to higher values (Figure 3.9c). By contrast, when more amount of solid TPA enters in the reactor (lower R_{EG}), lower temperatures promote the PET production increment.

Number-average molecular weight (in Figure 3.9d) and intrinsic viscosity (in Figure 3.9b) have very similar profiles. This resemblance is the result from IV calculation dependency of MW_N (as (2.21) shows). Analysing the profiles, both increase with higher ratios between EG and total feed and temperatures.

Chapter 4

Nonlinear Model Predictive Control of the Continuous Esterifier

The present chapter details the implementation of a nonlinear model predictive controller of the direct esterification unit of the PET production process. This strategy is applied by simulation based on the first principle model described in the previous chapters. Several tests were performed to show the significant advantages of NMPC application in processes that exhibit nonlinear behaviour.

4.1   NMPC Formulation

According to Asar (2004), reactors are normally one of the most important equipment in chemical industries. Only under an adequate controller performance it is possible to achieve the desired yields and to reduce side reactions, subject to process and quality constraints.

Linear model predictive control is based on linear mathematical models using time domain data to evaluate step response, to predict future process behaviour, and to determine the optimal manipulated variable profiles. Despite the fact that this control strategy has been successfully applied in processes whose dynamics is essential linear, it is not efficient for nonlinear processes (Dones et al., 2010). Nonlinear model predictive control (NMPC) based on first-principle models has the following advantages: the model is valid in a wider range of operating conditions, its parameters have a physical meaning easily interpretable by a chemical engineer, the predefined structure and relations between the input, state, and output variables reduce the time and effort of the so called step tests that are required in linear data based mod-

els. These benefits have been already tested in processes with stringent specifications such as
polymerisation (Manenti, 2011). Figure 4.1 shows the NMPC architecture.
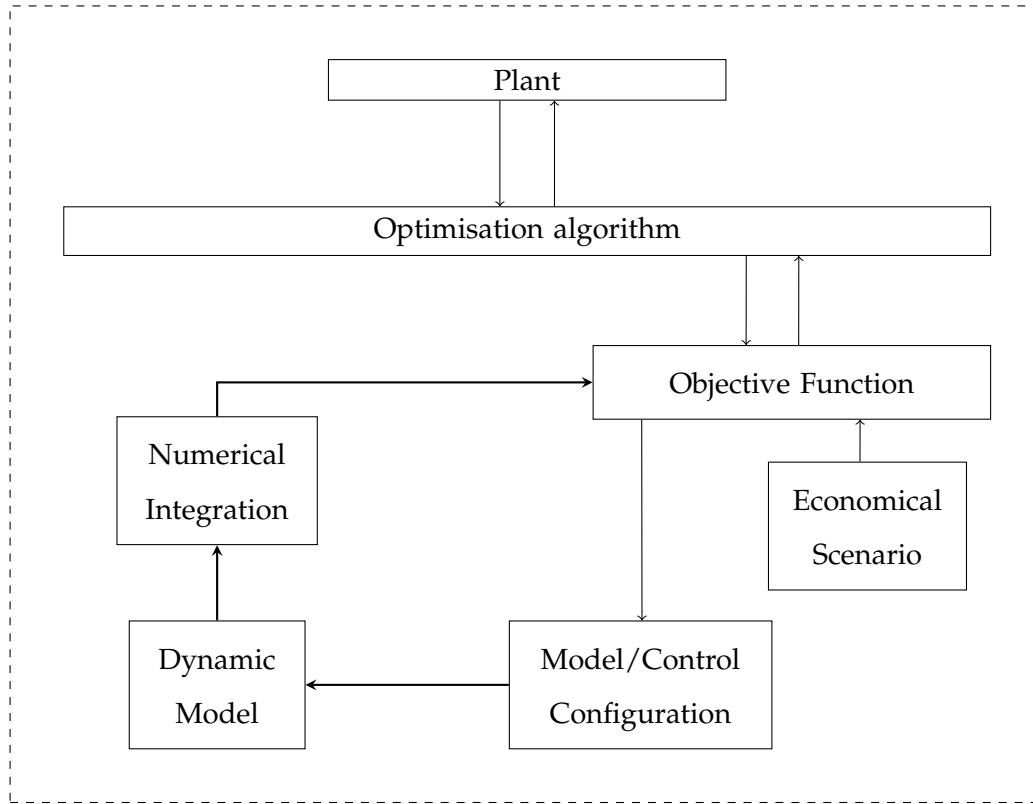
Figure 4.1: MNPC architecture. Adapted from Manenti (2011).

In a compact form, the process dynamic and the observation models can be mathematically
represented by

$$\dot{x} = f(x, u, d, \theta)\,, \tag{4.1a}$$

$$y = g(x)\,, \tag{4.1b}$$

with f and g twice continuously differentiable, where $x \in \mathbb{R}^{n_s}$ is the vector of state variables,
$u \in \mathbb{R}^{n_m}$ is the control vector, $d \in \mathbb{R}^{n_d}$ is the disturbance vector, $\theta \in \mathbb{R}^{n_\theta}$ is the parameter vector,
and $y \in \mathbb{R}^{n_o}$ is the vector of controlled variables.

In the present work, the NMPC problem to be solved at every sampling time k can be stated
as follows: for a certain predictive horizon of length p, given the current state measurements
and/or estimations, x_k, and the process model, compute the optimal control input sequence
over a control horizon of length m, $m \leqslant p$, that is $\{u_k^*, \ldots, u_{k+m-1}^*\}$, with $u_{k+i-1}^* = u_{k+m-1}^*$ for
$m < i \leqslant p$. This will result in an optimal sequence of state and controlled variables predictions

over p in the sense that they minimise the objective cost function of the NMPC problem. These optimal profiles can be denoted by $\{x^*_{k+1}, \ldots, x^*_{k+p}\}$ and $\{y^*_{k+1}, \ldots, y^*_{k+p}\}$, respectively.

In this work, the orthogonal collocation method NMPC based approach is similar to the formulation in Santos et al. (1995), which was developed from the Newton-type control formulations using sensitivity concepts described in Li and Biegler (1988) and Oliveira and Biegler (1995). Typically, the NMPC problem can be stated as the following discrete-time constrained dynamic optimisation problem:

$$\min_{X_k, U_k} \ \Psi\big(\tilde{Y}_k, U_k\big) \tag{4.2a}$$

$$\text{s.t. } \tilde{x}_{k+i} = \mathrm{f}(x_{k+i-1}, u_{k+i-1}, d, \theta, \Delta t), \ i = 1, \ldots, p \tag{4.2b}$$

$$\tilde{y}_{k+i} = \mathrm{g}(\tilde{x}_{k+i}), \ i = 1, \ldots, p \tag{4.2c}$$

$$u_{k+i-1} = u_{k+m-1}, \ m < i \leqslant p \tag{4.2d}$$

$$x_{k+i} - \tilde{x}_{k+i} = 0, \quad i = 1, \ldots, p-1 \tag{4.2e}$$

$$\tilde{X}_{\mathrm{L}} \leqslant \tilde{X}_k \leqslant \tilde{X}_{\mathrm{U}}, \ \tilde{Y}_{\mathrm{L}} \leqslant \tilde{Y}_k \leqslant \tilde{Y}_{\mathrm{U}}, \tag{4.2f}$$

$$X_{\mathrm{L}} \leqslant X_k \leqslant X_{\mathrm{U}}, \ U_{\mathrm{L}} \leqslant U_k \leqslant U_{\mathrm{U}}, \tag{4.2g}$$

where (4.2b) and (4.2c) are the discrete counterparts of (4.1), with Δt representing the sampling time period. The augmented vectors in (4.2) are defined as follows:

- $\tilde{Y}_k^{\mathrm{T}} = \left[\tilde{y}_{k+1}^{\mathrm{T}}, \cdots, \tilde{y}_{k+p}^{\mathrm{T}}\right]$ is the vector of the controlled predictions;

- $\tilde{X}_k^{\mathrm{T}} = \left[\tilde{x}_{k+1}^{\mathrm{T}}, \cdots, \tilde{x}_{k+p}^{\mathrm{T}}\right]$ is the vector of the state predictions;

- $X_k^{\mathrm{T}} = \left[x_k^{\mathrm{T}}, \cdots, x_{k+p-1}^{\mathrm{T}}\right]$ is the vector of the initial predictive state profiles;

- $U_k^{\mathrm{T}} = \left[u_k^{\mathrm{T}}, \cdots, u_{k+m-1}^{\mathrm{T}}\right]$ is the vector of the initial predictive control profiles.

As mentioned before, in this formulation the dynamic model is solved using a orthogonal collocation approach. This requires $p-1$ equality constraints (4.2e) in order to ensure the continuity of the state variables profiles over the predictive horizon. In (4.2e), $\tilde{x}_{k+i}$ is the state vector at $k+i$ obtained through the integration of the dynamic model inside each sampling time interval, with $t \in [t_{k+i-1}, t_{k+i}]$, using as initial conditions the nominal states and controls, x_{k+i-1} and u_{k+i-1}, respectively. This is why the decision variables of problem (4.2) are both the state and control trajectories, X_k and U_k, respectively. The subscripts $_\mathrm{L}$ and $_\mathrm{U}$ in the nonlinear constraints (4.2f) and in the decision variables bounds (4.2g) stand for *lower* and *upper* limit value respectively.

The rationale behind this formulation is: at every sampling time k determine the optimal solution, X_k^* and U_k^*, that minimise the cost function, such that the X_k^* and $\tilde{X}_k^*$ profiles match and are continuous over the predictive horizon, while satisfying all the problem constraints.

The NMPC formulation is complemented with the unscented Kalman filter (Julier and Uhlmann, 2004). At every time instant, based on the measurements, the filter provides the estimates of the state variables and of a set of the model parameters. The computational simulation framework features three independent and synchronised modules: the plant simulator module, the unscented Kalman filter module, and the NMPC module. Further details on this computational framework can be found in Brásio et al. (2013).

4.2 Control Problem Statement

The main goal is to obtain raw PET such that DEG composition is reduced avoiding quality problems in the final product. Besides, the controller has to perform production rate changes by adjusting the total flowrate of reactants. The nonlinear model predictive controller goal is to determine the best control policy establishing the optimal profiles for the manipulation variables over the given manipulated horizon in order to satisfy the setpoints of the controlled variables as well as the process operating constraints.

The control problem is composed by 5 controlled and 2 manipulated variables. The model contains 18 state variables: 1 related to the solid phase, 13 to the liquid phase, and 4 to the vapour phase. These 25 variables and their values at steady-state are listed in Table 4.1.

The cost function in (4.2a) is a quadratic function that incorporates the controlled and manipulated variables listed in Table 4.1 given by

$$
\Psi\left(\tilde{Y}_k, U_k\right) = \sum_{\ell=1}^{5} \lambda_\ell \sum_{i=1}^{p} \left(y_{\ell,\mathrm{sp},k+i} - \tilde{y}_{\ell,k+i}\right)^2 +
$$
$$
+ \sum_{\ell=6}^{7} \lambda_\ell \sum_{i=1}^{m} \left(u_{\ell,\mathrm{ref},k+i-1} - \tilde{u}_{\ell,k+i-1}\right)^2 , \tag{4.3}
$$

where λ_ℓ ($\ell = 1, \dots, 7$) are weighting scalars.

Table 4.1: List of controlled, manipulated, and state variables.

ℓ	Description	Symbol	Initial Value	Units
Controlled variables				
1	PET mass fraction in liquid phase	w_{PET}	26.184	$\%(m/m)$
2	DEG mass fraction in liquid phase	w_{DEG}	1.028	$\%(m/m)$
3	Intrinsic viscosity	IV	0.04818	dL g^{-1}
4	Number-average molecular mass	$\mathrm{MW_N}$	0.7565	kg mol^{-1}
5	Conversion	χ	24.00	$\%(m/m)$
Manipulated variables				
6	Total feed flowrate	$\dot{m}_{\mathrm{in}}$	4545	kg h^{-1}
7	Ratio between feed EG and total feed mass flowrates	R_{EG}	0.5	m/m
State variables				
8	AA molar holdup in vapour phase	$N_{\mathrm{vap,AA}}$	3.2161×10^{-2}	mol
9	DEG molar holdup in vapour phase	$N_{\mathrm{vap,DEG}}$	7.0827×10^{-1}	mol
10	EG molar holdup in vapour phase	$N_{\mathrm{vap,EG}}$	1.6718×10^{2}	mol
11	W molar holdup in vapour phase	$N_{\mathrm{vap,W}}$	6.1850×10^{1}	mol
12	AA molar holdup in liquid phase	$N_{\mathrm{liq,AA}}$	4.6820×10^{-2}	mol
13	DEG molar holdup in liquid phase	$N_{\mathrm{liq,DEG}}$	7.2372×10^{1}	mol
14	EG molar holdup in liquid phase	$N_{\mathrm{liq,EG}}$	4.2275×10^{3}	mol
15	TPA molar holdup in liquid phase	$N_{\mathrm{liq,TPA}}$	4.9839×10^{1}	mol
16	W molar holdup in liquid phase	$N_{\mathrm{liq,W}}$	8.4827×10^{2}	mol
17	PET molar holdup in liquid phase	$N_{\mathrm{liq,PET}}$	1.8439×10^{3}	mol
18	B-DEG molar holdup in liquid phase	$N_{\mathrm{liq,B\text{-}DEG}}$	9.7723×10^{1}	mol
19	B-EG molar holdup in liquid phase	$N_{\mathrm{liq,B\text{-}EG}}$	4.7750×10^{3}	mol
20	B-TPA molar holdup in liquid phase	$N_{\mathrm{liq,B\text{-}TPA}}$	6.4071×10^{3}	mol
21	T-EG molar holdup in liquid phase	$N_{\mathrm{liq,T\text{-}EG}}$	3.3163×10^{3}	mol
22	T-TPA molar holdup in liquid phase	$N_{\mathrm{liq,T\text{-}TPA}}$	3.0829×10^{2}	mol
23	T-VIN molar holdup in liquid phase	$N_{\mathrm{liq,T\text{-}VIN}}$	2.2431×10^{-3}	mol
24	T-DEG molar holdup in liquid phase	$N_{\mathrm{liq,T\text{-}DEG}}$	6.3094×10^{1}	mol
25	TPA molar holdup in solid phase	$N_{\mathrm{sol,TPA}}$	4.5454×10^{3}	mol

4.3 Results and Discussion

The dynamic first-principle model studied in previous chapters is used in the advanced process control application. All simulations were obtained with a predictive horizon of $p = 30$, a control horizon of $m = 15$, and a sampling time of 1 min.

4.3.1 Computational Implementation

In this study, the NMPC system called Plantegrity® comprising a controller module, a state
and parameter estimator module, and a communication module was used to implement the
tests. The two additional modules are important. While the communication module provides
integration of NMPC with a DCS (distributed control system) or PLC (programmable logic con-
troller) controlling the plant, the estimator module estimates the states variables (to initialise
the integration of the model equations within the NMPC module) and some model parameters
(as means of compensation for plant/model mismatch and/or unmeasured disturbances). In
the case of simulation scenarios as the present study, the communication module is replaced
with a plant simulator.

Plantegrity® workflow is as follows:

- the communication module or the plant simulator provide process measurements to the
  state and parameter estimator;

- using these data and the process model, the estimator obtains the best estimates of the
  state vector and of parameters;

- the NMPC module solves the optimisation problem and determines the optimum values
  for the manipulated variables;

- these values are passed over to the communication module for implementation in the
  plant or, in the case of simulation, are used in the simulator to carry out the next simula-
  tion step.

Plantegrity® contains also a multiplatform user interface for easy handling of setpoint, ref-
erence and constraint profiles and weights. It also serves to preform data analysis and trending
framework. Figure 4.2 provides the interface configuration used in the present work.

Plantegrity® was installed on a Intel Core i5 with a 3.20GHz processor running the GNU
Linux operating system. The nonlinear first principle model was translated, with necessary
adaptations, from GNU Octave to C++ because the latter is the core language of the NMPC
system. An example of the developed code is presented in Appendix D.
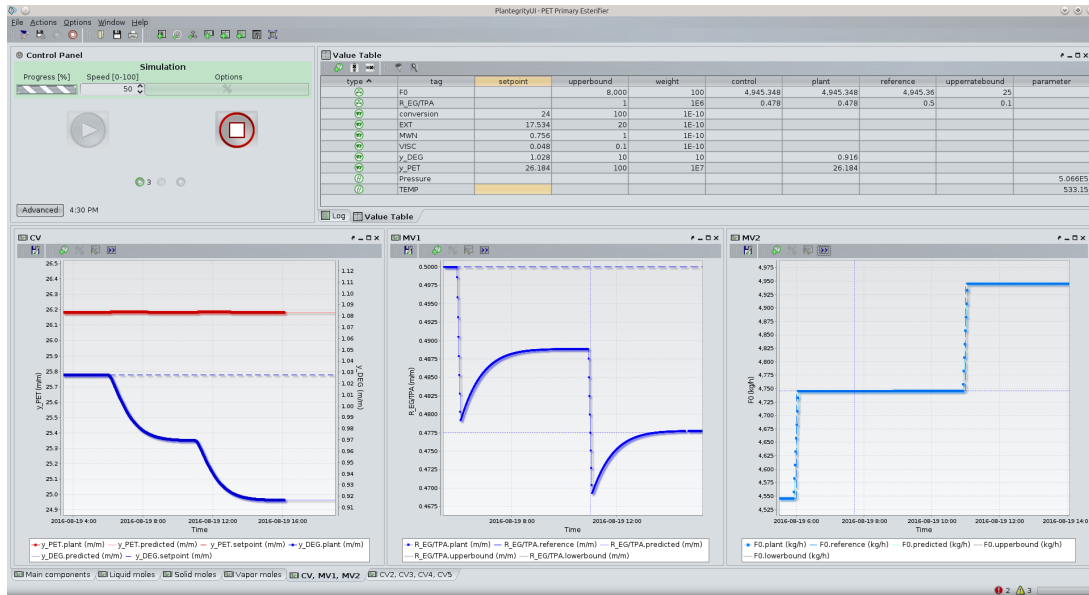
Figure 4.2: NMPC platform interface.

4.3.2 Simulations

Distinct system responses using NMPC were evaluated. Firstly, Test A shows the NMPC performance to a negative change in the DEG composition setpoint. In Test B, PET composition is maintained while the total feed flowrate is increased $200 \, \text{kg} \, \text{h}^{-1}$ in two steps. Test C gives the comparison between the traditional control and the NMPC when a disturbance in the total feed flowrate is made. In each test, DEG and PET mass fractions, conversion, number-average molecular weight, and intrinsic viscosity profiles (controlled variables) are shown. In addition, manipulated variables profiles are also illustrated. All tests consider the steady-state identified in Table 4.1 as the initial state, at a temperature equal to $260\,^{o}\text{C}$. NMPC control parameters are depicted in Table 4.2.

Test A

The first test shows how NMPC control performs when a new product specification in DEG composition is imposed. Figures 4.3 and 4.4 illustrate controlled and manipulated variables profiles evolution, respectively.

The production starts in a control mode that maintains the initial values of the controlled and manipulated variables (Table 4.2), because the weights, λ_l, associated with the number-average molecular weight and the conversion are set to a small value of 10^{-10} and the mass fractions of PET and DEG have similar importance (weights are set to 10^1).

47

Table 4.2: NMPC control parameters.

	λ_l	LB	UB	LRB	URB	Setpoint	Reference
Controlled variables							
w_{PET}, %(m/m)	10^1	0.000	100.000	–	–	26.184	–
w_{DEG}, %(m/m)	10^1	0.000	10.000	–	–	1.028	–
IV, dL g^{-1}	10^{-10}	0.010	0.100	–	–	0.048	–
MW_{N}, kg mol^{-1}	10^{-10}	0	100	–	–	24	–
χ, %(m/m)	10^{-10}	0.000	1.000	–	–	0.756	–
Manipulated variables							
R_{EG}, (m/m)	10^6	0.30	1.00	-0.10	0.10	–	0.50
$\dot{m}_{\text{in}}$, kg h^{-1}	10^4	1000	8000	-25	25	–	4545

As can be seen in Figure 4.4, the system is initially under regulatory control with a total feed flowrate of 4545 kg h^{-1} and a R_{EG} of 0.5. The production run starts in a control mode that maintains PET composition equals to 1.028 %(m/m) and DEG composition equals to 26.184 %(m/m). At 0.24 h, the new objective is introduced in the controller: DEG mass fraction setpoint is set to 0.9 %(m/m) as Figure 4.3a shows, while the total feed flowrate is maintained constant. To implement these new objectives, DEG mass fraction weight was redefined to 10^7 and ratio R_{EG} weight was relaxed to 10^4.

Starting at a value of 0.5, R_{EG} is immediately reduced until its lowerbound at 0.3 and then increased stabilising at 0.4680 (Figure 4.4b). This undershoot in R_{EG} variable influences controlled variables profiles that show an overshoot in the transition to the new steady-state. Despite of the increment in PET mass fraction is almost 1 %(m/m), the conversion reduces from 23.82 to 23.58 %(m/m) as Figures 4.3b and 4.3c show. This happens due to the R_{EG} reduction. The conversion decreasing means that the PET production is also reduced as one may infer by analysis of (3.4). At the same time, PET mass fraction increases because the limiting reactant EG was lowered reducing the reactions extension and, consequently, producing smaller quantities of all components. Number-average molecular weight and intrinsic viscosity properties also show a slightly increase in the last stage of the closed-loop simulation.

Test B

The objective in this test is to check the controller performance when total feed flowrate changes are carried out in a pre-scheduled way maintaining the product quality in the primary esterifier outlet. The product quality is maintained through the PET mass fraction in the liquid

(a) DEG mass fraction.

(b) PET mass fraction.

(c) Conversion.

(d) Number-average molecular weight.

(e) Intrinsic viscosity.
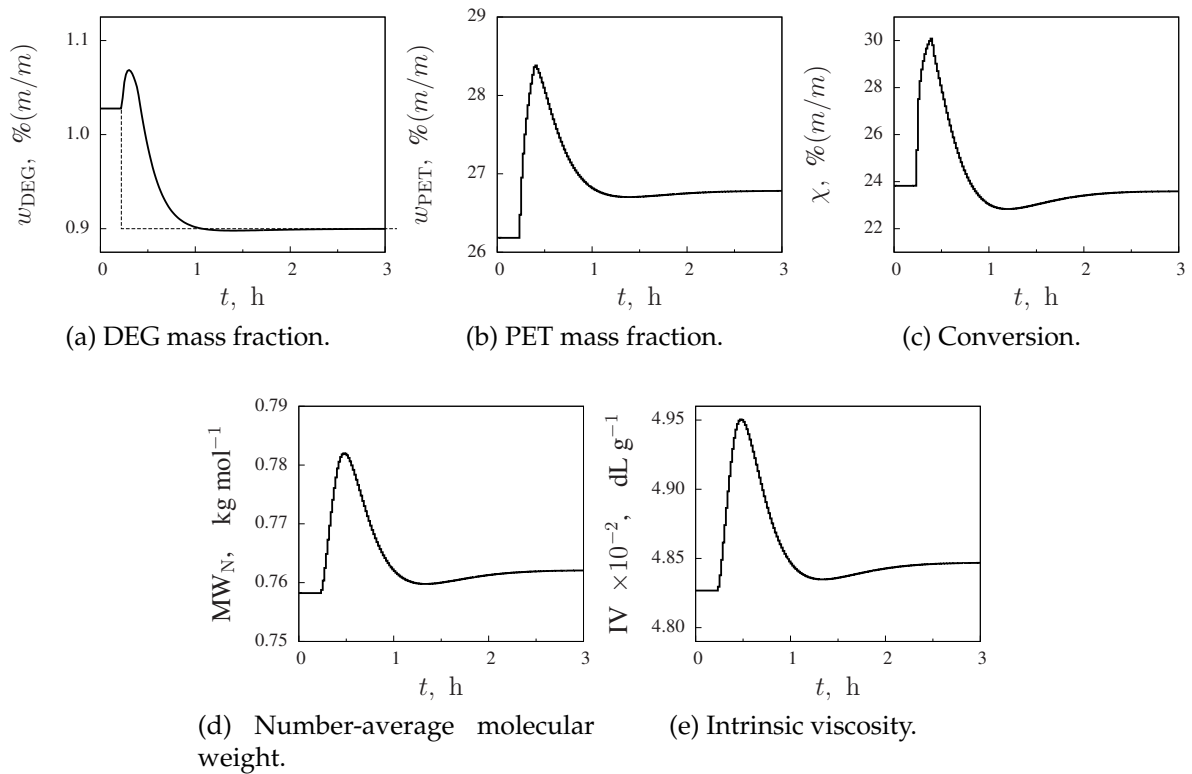
Figure 4.3: Test A, closed-loop profiles of controlled variables.

(a) total feed flowrate.

(b) Ratio between EG and total feed flowrates.
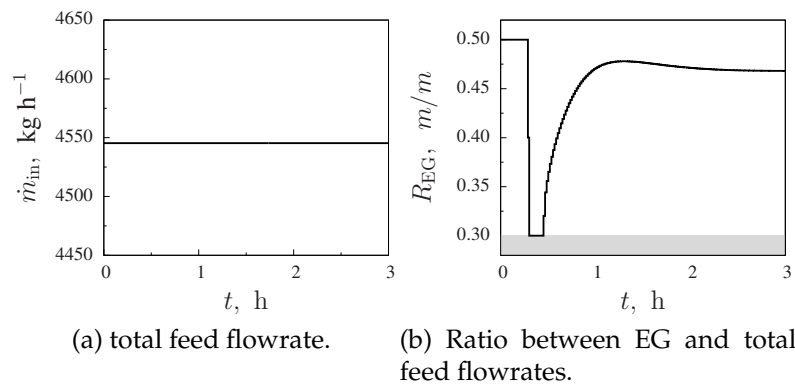
Figure 4.4: Test A, closed-loop profiles of manipulated variables.

phase. Figures 4.5 and 4.6 show the controlled and manipulated variables profiles.

Initially, the NMPC control configuration is performed as Table 4.2 shows. total feed flowrate increment of $400 \, \text{kg} \, \text{h}^{-1}$ is made in two steps. The first increment of $200 \, \text{kg} \, \text{h}^{-1}$ is made at $0.92 \, \text{h}$ and the second one at $5.9 \, \text{h}$ as is illustrated in Figure 4.6a. Before introducing the first increment, the weight of the PET mass fraction objective in the cost function (4.3) is increased from 10^1 to 10^7. The weight of the total feed flowrate is also changed to 10^2.

The objective of maintaining the PET mass fraction at the setpoint is accomplished (see

Figure 4.5b) by decreasing the ratio between EG and the total feed flowrate (Figure 4.6b). At the same time, DEG mass fraction and conversion reduced their values as well as the properties.

(a) DEG mass fraction. (b) PET mass fraction. (c) Conversion.

(d) Number-average molecular weight. (e) Intrinsic viscosity.
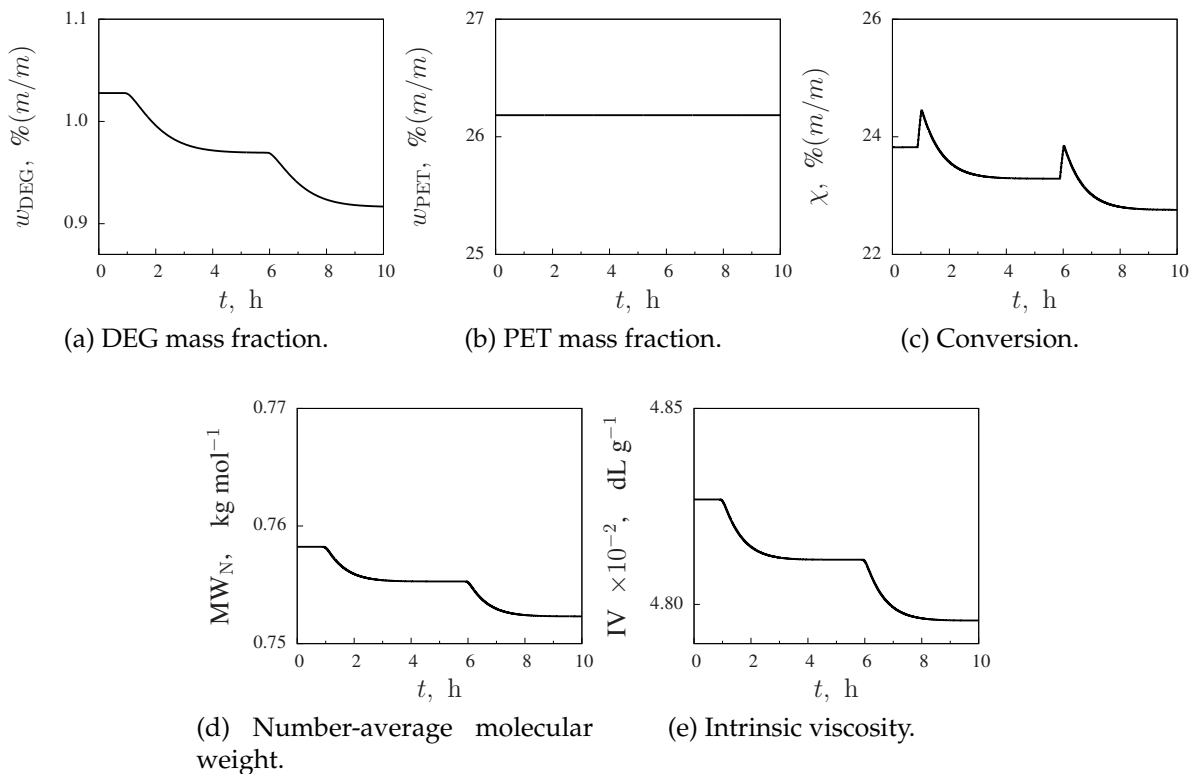
Figure 4.5: Test B, closed-loop profile of controlled variables.

(a) total feed flowrate. (b) Ratio between EG and total feed flowrates.
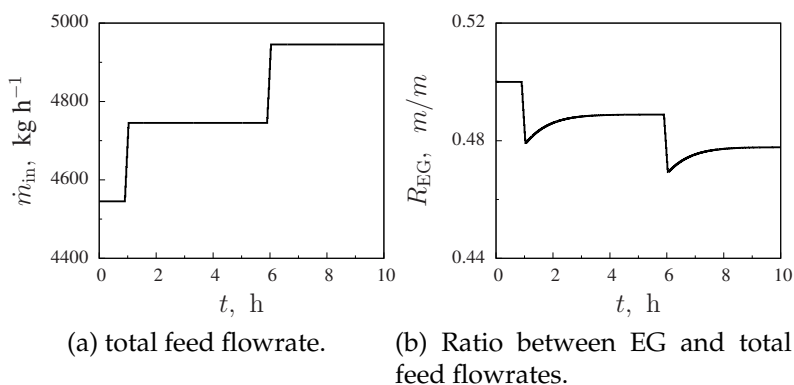
Figure 4.6: Test B, closed-loop profile of manipulated variables.

Test C

This experiment exemplifies the differences between the traditional control and NMPC during step transition in the total feed flowrate from 4545 to 4745 kg h^{-1} around the 3 h. Traditional

control resorts to the control of the ratio R_{EG} as a constant value. With the change of the total feed flowrate, the traditional control remains unaware of the evolution of the other key process variables, and maintains the ratio constant which means that for, the $200\,\mathrm{kg\,h^{-1}}$ increment in the total feed flowrate, the traditional control raises the EG flowrate exactly in $100\,\mathrm{kg\,h^{-1}}$. To simulate this scenario, the NMPC system was used with the configuration presented in Table 4.2. Initially, the same configuration was used and, before the step change in the total feed flowrate, PET mass fraction weight was changed to 10^7.

Graphical results are portrayed in Figures 4.7 and 4.8 for controlled and manipulated variables, respectively. Figure 4.7 clearly shows the differences between traditional control and NMPC, mainly in PET mass fraction variable. With NMPC, its composition is maintained at the specified setpoint, while traditional control presents a decrease of $0.3\,\%(m/m)$ as is depicted in Figure 4.7b. In order to maintain PET mass fraction, NMPC reduces the amount of feed EG in the reactor (the steady-state value of R_{EG} is changed to 0.489) as shown in Figure 4.8b, while the traditional method makes no changes to this variables. In addiction, DEG mass fraction is reduced which is positive given its consequences in final product quality. Relatively to PET properties, the MW_N and IV steady-state values are slightly higher in traditional control (see

(a) DEG mass fraction.

(b) PET mass fraction.

(c) Conversion.

(d) Number-average molecular weight.

(e) Intrinsic viscosity.
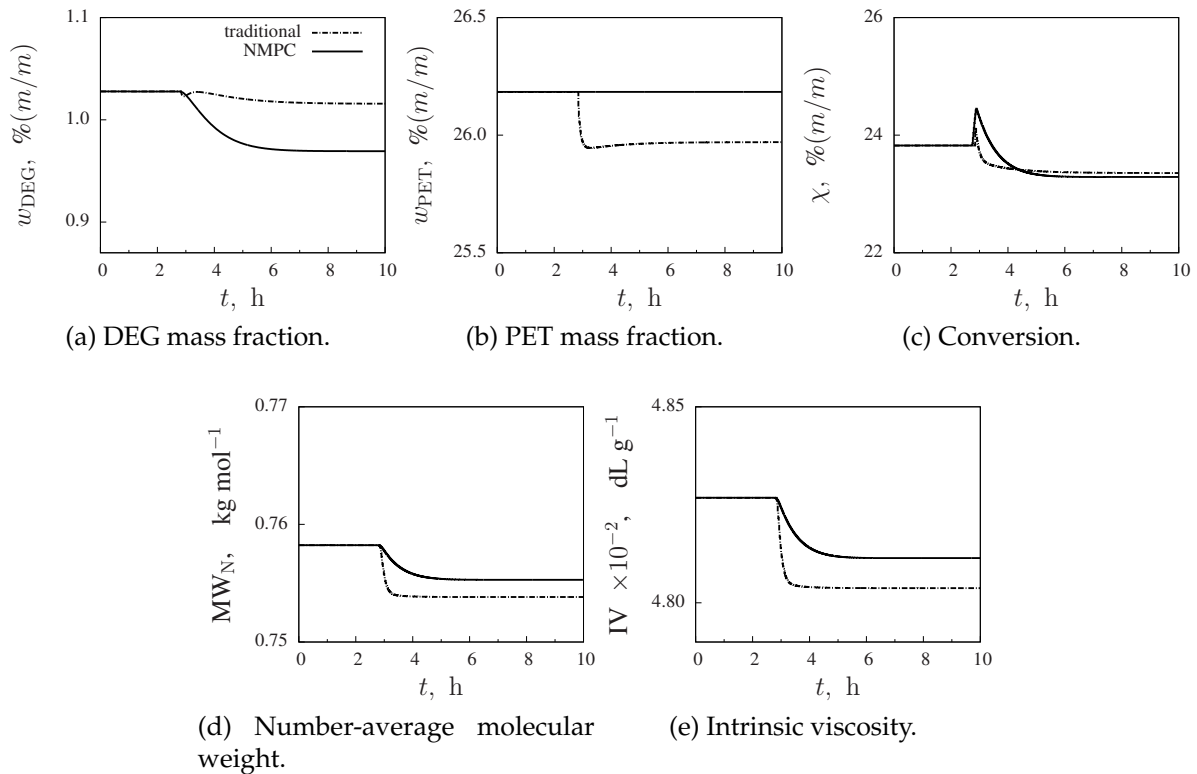
Figure 4.7: Test C, closed-loop profile of controlled variables

51

(a) total feed flowrate.

(b) Ratio between EG and total feed flowrates.
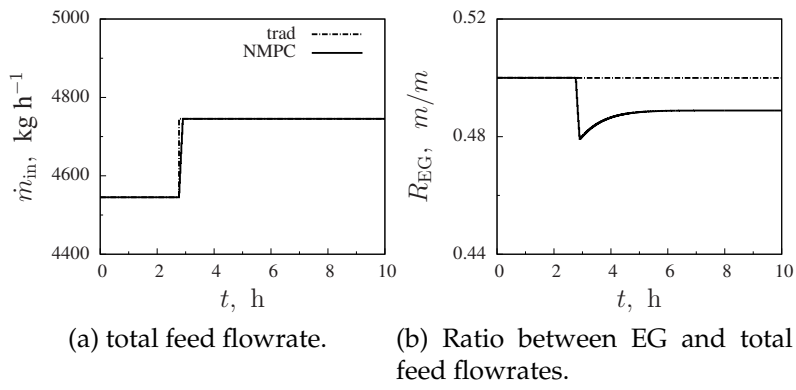
Figure 4.8: Test C, closed-loop profile of manipulated variables.

Figures 4.7d and 4.7e).

Chapter 5

Conclusions and Future Work

In this chapter, the main contributions of the present dissertation are outlined. Additionally, possible future research directions of the esterification reactor as well as of the entire PET plant modelling and control are highlighted.

5.1 Main contributions

5.1.1 Numerical Implementation and Simulation of Reaction Kinetics Model

Chapter 2 comprises the mathematical modelling and computational implementation in GNU Octave of the primary esterifier where ethylene glycol and terephthalic acid firstly react to produce PET. The continuous TPA based technology for producing PET was considered as it allows faster reactions rates, better yields, less hazardous side product and substantial costs reduction. The complex polymerisation process comprises several stages characterised by a strong nonlinear behaviour and, consequently, its modelling is not a trivial task. The segment-based Seavey and Liu (2009) mathematical model was chosen to describe the dynamic behaviour of the liquid phase in the primary esterifier where PET is initially produced. The kinetic model of the direct esterification reaction was incorporated into a batch reactor model and the case study of reactor start-up was studied. Simulated results were compared with the literature showing a good agreement.

5.1.2   Modelling of a Continuous Dynamic Esterifier

Kinetic reaction validation was followed by the dynamic mathematical modelling of the continuous primary esterifier based on first principles and its computational implementation in GNU Octave. Considering vapour, liquid, and solid phases, the multi-compartmental model considers: (1) reaction only occurring in liquid phase, (2) solid terephthalic acid is transferred by dissolution to the liquid phase, and (3) liquid W, EG, AA and DEG are transferred by diffusion from the liquid to the vapour phase. Since the dynamic model is characterised by discontinuous nonlinear equations, two approaches based on discontinuities smoothing were applied to the discontinuity points in order to the model becomes solvable using continuous optimisation tools which is very important to the real-time optimisation and the advanced process control application. Fed by liquid ethylene glycol and solid terephthalic acid, the reactor start-up was studied comparing, at the same time, the generated results with the literature. Although the discontinuities smoothing techniques slightly changed the profiles in some simulation zones, the generated results showed a good agreement with those of the literature.

Additionally, a study on the reactor operating conditions was also accomplished, valid for ratios between feed ethylene glycol and total feed mass flowrate in the range of [0.1, 0.9] and temperatures in the range of [245, 285]°C. The obtained profiles for conversion, intrinsic viscosity, molar PET production rate, and number-average molecular weight confirmed the strong nonlinear behaviour of the model and showed that the optimal operation point is very dependent on the production objectives.

5.1.3   Nonlinear Model Predictive Control of the Continuous Esterifier

Chapter 4 presents the application of a nonlinear predictive controller for the optimisation of the primary esterification unit of the PET production process using the Plantegrity® model predictive control system. In an initial phase, the nonlinear first principle model of the continuous esterifier described in the previous chapters was translated to C++ language because it is the core language of Plantegrity®. In this control configuration there are 5 controlled, 2 manipulated, and 19 state variables . Three distinct tests were evaluated by simulation to demonstrate the system capabilities of performing regulatory and servo control. In a first test, the NPMC performance was tested while the setpoint of the final DEG mass fraction was subjected to a

negative step. The second test checked the controller performance in the presence of several disturbances in the total feed flowrate. Finally, third test compares the traditional control with the NMPC in the presence of a disturbance in the total feed flowrate.

The NMPC controller determined successfully the optimal profiles of the process variables improving the process economic performance while complying with final product specifications. Despite the scarcity of NMPC applications to PET plants reported in the literature, its benefits were here demonstrated, exhibiting good regulatory and servo control performances.

5.2 Future Work

Based in the reflection and inspiration from the study present in this dissertation, further refinements and potential research directions may be investigated.

- **Control of DEG segments incorporated into the polymeric chain** PET polymer chain is composed by bounded and terminal segments of DEG which molar percentage in the polymeric chain, usually around the 1.0 and 3.6 %(n/n), must be limited in order to minimise their influence in the polymer properties (Romão et al., 2009). Although this dissertation focuses on the DEG present in the liquid phase, DEG inside the polymeric chain must also be minimised in order to guarantee final polymer properties. Molar fraction of DEG incorporated into the polymer is calculated through

$$x_{\text{DEG}}^{\text{polymeric chain}} = \frac{N_{\text{liq,B-DEG}} + N_{\text{liq,T-DEG}}}{\sum_{i \in \mathcal{I}} N_{\text{liq},i} + \sum_{j \in \mathcal{J}} N_{\text{liq},j}}, \qquad (5.1)$$

  where $\mathcal{I} = \{\text{B-DEG, B-EG, B-TPA}\}$ and $\mathcal{J} = \{\text{T-DEG, T-EG, T-TPA, T-VIN}\}$. The evolution of DEG molar fraction corresponding to the simulation study performed in Section 3.3.2 is depicted in Figure 5.1. For the steady-state, the molar fraction of DEG incorporated into the polymer assumes a value near 1.0 %(n/n) which is inside the range of values identified by the literature. However, one more esterification step and the melt and solid phases polymerisation will follow increasing this amount of DEG. The continuous reactor control considering this quality product constraint could identify the optimal profiles of the operation conditions for the minimisation of the DEG incorporation into the polymeric chain.
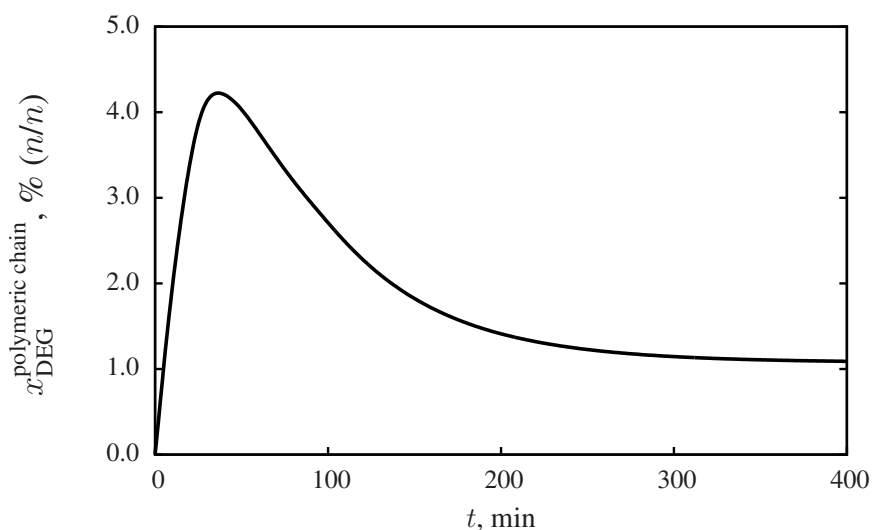
Figure 5.1: Mass fraction of DEG incorporated into the polymeric chain.

- **Modelling of the reactor energy balance and temperature control** The main goal it to develop the energy balance to the continuous reactor based on first principles. After a simulation study of this more complete system, the reactor temperature could be introduced into the developed NMPC system as manipulated variable, thus providing more degrees of freedom to the controller.

- **Modelling of the distillation column and the secondary esterification** A distillation column and a secondary esterifier are connected to the primary esterifier. While the distillation column separates the evaporated EG from the other vapour components and introduced it again into the reactor, the secondary esterifier complete the esterification reaction. The mathematical modelling of these two important units of the PET production process would bring more knowledge of the influence of this reaction on the key process variables.

- **Modelling and control of the melt and solid phases polymerisation** After the esterification study is completed, other two important production steps may be explored. As described in the introduction, melt and solid phases polymerisation are the following steps. Melt phase polymerisation is usually done in the low, intermediate, and high polymerisation and solid phase polymerisation in two crystallisers and one solid phase reactor. The study on these steps would complete the PET production process modelling. The implementation of the developed model in the NMPC system and its application into a real plant would verify the economical benefits highlighted in the literature.

Bibliography

Abbo, A. J. and Sloan, S. W. (1995). A smooth hyperbolic approximation to the Mohr-Coulomb yield criterion. *Computers & Structures*, 54(3):427–441.

Ahn, Y.-C. and Choi, S.-M. (2003). Analysis of the esterification process for poly(ethylene terephthalate). *Macromolecular Research*, 11(6):399–409.

Allgöwer, F., Findeisen, R., and Nagy, Z. K. (2004). Nonlinear model predictive control: From theory to application. *Journal of the Chinese Institute of Chemical Engineers*, 35(3):299–315.

Asar, I. (2004). Model Predicative Control (MPC) Performance for Controlling Reaction Systems. Master's thesis, Middle East Technical University.

Balakrishna, S. and Biegler, L. T. (1992). Targeting strategies for the synthesis and energy integration of nonisothermal reactor networks. *Industrial & Engineering Chemistry Research*, 31(9):2152–2164.

Banat, Y. and Abu, E.-R. Z. (2001). A Technical and Economic Feasibility Study of : Production of Polyethylene Terephthalate by Direct Esterification Using Pervaporation. Technical Report April, University of Twente, Faculty of Chemical Technology.

Bartolome, L., Imran, M., Cho, B. G., Al-Masry, W. A., and Kim, D. H. (2012). Recent developments in the chemical recycling of pet. *Material Recycling - Trends and Perspectives*.

Besnoin, J.-M. and Choi, K. Y. (1989). Identification and characterization of reaction byproducts in the polymerization of polyethylene terephthalate. *Journal of Macromolecular Science, Part C*, 29(1):55–81.

Bhaskar, V., Gupta, S. K., and Ray, A. K. (2001). Modeling of an industrial wiped film poly(ethylene terephthalate) reactor. *Polymer Reaction Engineering*, 9(2):71–99.

Brásio, A. S., Romanenko, A., Leal, J., Santos, L. O., and Fernandes, N. C. (2013). Nonlinear model predictive control of biodiesel production via transesterification of used vegetable oils. *Journal of Process Control*, 23(10):1471 – 1479.

Brásio, A. S. R., Romanenko, A., and Fernandes, N. C. P. (2014). Stiction detection and quantification as an application of optimization. In Murgante, B., Misra, S., Rocha, A., Torre, C., Rocha, J., Falcão, M., Taniar, D., Apduhan, B., and Gervasi, O., editors, *Computational Science and Its Applications – ICCSA 2014*, volume 8580 of *Lecture Notes in Computer Science*, pages 169–179. Springer International Publishing.

Chen, C. C. (1993). A segment-based local composition model for the gibbs energy of polymer solutions. *Fluid Phase Equilibria*, 83(C):301–312.

Chen, J.-W. and Chen, L.-W. (1998). The kinetics of diethylene glycol formation in the preparation of polyethylene terephthalate. *Journal of Polymer Science Part A: Polymer Chemistry*, 36(17):3073–3080.

Dones, I., Manenti, F., Preisig, H. A., and Buzzi-Ferraris, G. (2010). Nonlinear model predictive control: A self-adaptive approach. *Industrial & Engineering Chemistry Research*, 49(10):4782–4791.

Hindmarsh, A. C. (2006). Serial fortran solvers for ode initial value problems. http://www.cplusplus.com/info/description/. Acessed 3 August 2016.

IBISWorld (2016). Global Plastic Product & Packaging Manufacturing: Market Research Report. http://www.ibisworld.com/industry/global/global-plastic-product-packaging-manufacturing.html. Online, Accessed at 17 May 2016.

Immanuel, C. D. (2000). Optimization of the first stage continuous reactor-sequence in polyester manufacture from purified terephthalic acid. *Journal of Polymer Engineering*, pages 51–75.

Julier, S. J. and Uhlmann, J. K. (2004). Unscented filtering and nonlinear estimation. *Proceedings of the IEEE*, 92(3):401–422.

Kang, Chang-Kwon; Lee, B. C. and Ihm, D. W. (1997). A Simulation Study on Continuous Direct Esterification Process for Polyethylene terephthalate) Synthesis. *Applied Polymer Science*, pages 163–174.

Kang, C.-K., Lee, B. C., and Ihm, D. W. (1996). Modeling of semibatch direct esterification reactor for poly(ethylene terephthalate) synthesis. *Journal of Applied Polymer Science*, 60(11):2007–2015.

Kayihan, A. and Doyle III, F. J. (2000). Friction compensation for a process control valve. *Control Engineering Practice*, 8(7):799–812.

Kim, I. S., Woo, B. G., Choi, K. Y., and Kiang, C. (2003). Two-Phase Model for Continuous Final-Stage Melt Polycondensation of Poly(ethylene terephthalate). III. Modeling of Multiple Reactors with Multiple Reaction Zones. *Journal of Applied Polymer Science*, 90(4):1088–1095.

Kim, J.-Y., Kim, H.-Y., and Yeo, Y.-K. (2001). Identification of kinetics of direct esterification reactions for PET synthesis based on a genetic algorithm. *Korean Journal of Chemical Engineering*, 18(4):432–441.

Kumar, A., Sukthankar, V. K., Vaz, C. P., and Gupta, S. K. (1984). Optimization of the trans-esterification stage of polyethylene terephthalate reactors. *Polymer Engineering & Science*, 24(3):185–193.

Kumar, A., Wahal, S., and Sastri, S. (1986). Modelling of intramolecular reactions in the step-growth polymerization of multifunctional monomers. *Polymer*, 27(4):583–591.

Li, W. C. and Biegler, L. T. (1988). Process control strategies for constrained nonlinear systems. *Ind. Eng. Chem. Res.*, 27:1421–1433.

Luo, N. and Qian, F. (2012). Parameter estimation of industrial pet reactor using multi-objective kernel density estimation of distribution algorithm. *Asia-Pacific Journal of Chemical Engineering*, 7(5):783–794.

Maca, M. (2005). A Framework for NonLinear Model Predictive Control. Master's thesis, Czech Technical University in Prague Faculty of Electrical Engineering Department of Contro Engineering.

Manenti, F. (2011). Considerations on nonlinear model predictive control techniques. *Computers & Chemical Engineering*, 35(11):2491–2509.

Manenti, F. and Rovaglio, M. (2008). Integrated multilevel optimization in large-scale polyethylene terephthalate plants. *Industrial and Engineering Chemistry Research*, 47(1):92–104.

Maria, A. (1997). Introduction to modeling and simulation. In *Proceedings of the 29th Conference on Winter Simulation*, WSC '97, pages 7–13, Washington (USA). IEEE Computer Society.

Mazloom, M., Rafizadeh, M., Haddadi-asl, V., and Pakniat, M. (2007). Synthesis and Mathematical Modelling of Polyethylene Terephthalate via Direct Esterification in a Laboratory Scale Unit. *Iranian Polymer Journal*, 16(9):587–596.

Oliveira, N. M. C. and Biegler, L. T. (1995). Newton-type Algorithms for Nonlinear Process Control. Algorithm and Stability Results. *Automatica*, 31(2):281–286.

Patel, H., Feix, G., and Schomäcker, R. (2007a). Influence of reaction pressure on semibatch esterification process of poly(ethylene terephthalate) synthesis. *Macromolecular Symposia*, 259:65–75.

Patel, H., Feix, G., and Schomäcker, R. (2007b). Modeling of Semibatch Esterification Process for Poly(ethylene terephthalate) Synthesis. *Macromolecular Symposia*, pages 502–512.

Plastics Industry Trade Association (2016). A Few Fast Facts on... Plastics and the Economy. http://www.plasticsindustry.org/AboutPlastics/. Online, Accessed at 17 May 2016.

Processing, P. (2009). Acetaldehyde a.a. in poly(ethylene terephthalate) processing. http://polymerprocessing.blogspot.pt/2009/04/acetaldehyde-aa-in-polyethylene.html. Acessed 3 August 2016.

Romão, W., Spinaci, M. A. S., and Paoli, M.-A. D. (2009). Poli(tereftalato de etileno), PET: uma revisão sobre os processos de síntese, mecanismos de degradação e sua reciclagem. *Polímeros*, 19:121 – 132.

Santos, L. O., Oliveira, N. M. C., and Biegler, L. T. (1995). Reliable and Efficient Optimization Strategies for Nonlinea Model Predictive Control. In Rawlings, J. B., editor, *Proc. of DYCORD+'95, Helsingør, Denmark*, pages 33–38, Oxford. Elsevier Science.

Scheirs, J. and Long, T. E. (2003). *Modern Polyesters: Chemistry and Technology of Polyesters and Copolyesters*. Wiley Series in Polymer Science.

Seavey, K. and Liu, Y. (2009). *Step-Growth Polymerization Process Modeling and Product Design*. Wiley.

Sloan, S. W. and Booker, J. R. (1986). Removal of singularities in Tresca and Mohr-Coulomb yield functions. *Communications in Applied Numerical Methods*, 2(2):173–179.

SRI (2016). PET. http://www.sri-bv.com/pet/. Online, Accessed at 18 May 2016.

Todd Johnson (2016). Polyethylene Terephthalate. http://composite.about.com/od/Plastics/a/What-Are-Pet-Plastics.htm. Online, Accessed at 17 May 2016.

Yamada, T. and Imamura, Y. (1985). A mathematical model for computer simulation of a direct continuous esterification process between terephthalic acid and ethylene glycol: Part1. Model development. *Polymer-Plastics Technology and Engineering*, 5(7-8):811–876.

Yamada, T. and Imamura, Y. (1986). A mathematical model for computer simulation of a direct continuous esterification process between terephthalic acid and ethylene glycol: Part II:Raction and rate constants. *Polymer-Plastics Technology and Engineering*, 26(10):811–876.

Yamada, T. and Imamura, Y. (1988). A mathematical model for computer simulation of a direct continuous esterification process between terephthalic acid and ethylene glycol. *Polymer Engineering & Science*, 28(6):385–392.

Yamada, T. and Imamura, Y. (1989). Simulation of Continuous Direct Esterification Process between Terephthalic Acid and Ethylene Glycol. *Polymer-Plastics Technology and Engineering*, 28(7-8):811–876.

Appendices

Appendix A

Properties Constants

Table A.1: Component molecular weight ([Seavey and Liu, 2009]).

Component i	MW_i, kg mol^{-1}
AA	4.405×10^{-2}
DEG	1.061×10^{-1}
EG	6.207×10^{-2}
TPA	1.661×10^{-1}
W	1.802×10^{-2}
PET monomer	1.922×10^{-1}
B-DEG	1.040×10^{-1}
B-EG	6.010×10^{-2}
B-TPA	1.490×10^{-1}
T-EG	6.110×10^{-2}
T-TPA	1.490×10^{-1}
T-VIN	4.305×10^{-2}
T-DEG	1.050×10^{-1}

Table A.2: Component vapour pressure parameters (Seavey and Liu, 2009).

Component i	A_i	B_i	C_i	D_i	E_i	F_i	G_i
AA	206	-8.48×10^3	-3.15×10^1	4.63×10^{-2}	1.00	150.2	461.0
DEG	74.6	-1.06×10^4	-6.82×10^0	9.10×10^{-18}	6.00	262.7	680.0
EG	195	-1.46×10^4	-2.54×10^1	2.01×10^{-5}	2.00	260.2	645.0
TPA	59.8	-1.10×10^3	-8.67×10^0	4.63×10^{-2}	1.00	63.15	126.1
W	-4010	-1.77×10^5	-6.30×10^2	-5.12×10^{-1}	1.00	523.0	700.2
PET	73.6	-7.26×10^3	-7.30×10^0	4.17×10^{-6}	2.00	273.2	647.1

Table A.3: Component liquid density parameters (Seavey and Liu, 2009).

Component	A_i	B_i	C_i	D_i	E_i	F_i
AA	1.670	0.260	461.000	0.278	150.150	461.000
DEG	0.848	0.264	680.000	0.197	262.700	680.000
EG	1.340	0.255	645.000	0.172	260.150	645.000
W	5.460	0.305	647.000	0.081	273.160	333.150

Table A.4: Binary interaction parameters (Seavey and Liu, 2009). All the interactions not specified are set to zero.

i	j	$A_{i,j}$	$A_{j,i}$	$B_{i,j}$	$B_{j,i}$
EG	W	-0.0567	0.348	-147	34.8
TPA	W	-6.52	6.52	2390	-1000
EG	TPA	-3.85	-5.16	1230	3770
W	DEG	0.0	0.0	18.385	-43.805
W	AA	0.0	0.0	246.6	505.6
EG	DEG	-2.806	-0.583	2320.7	-312.2
EG	AA	0.0	0.0	-172.9	334.1
TPA	DEG	0.0	0.0	562.3	-330.8
DEG	AA	0.0	0.0	-337.8	-207.4
TPA	AA	0.0	0.0	1068.2	-633.4

A.2

Appendix B

Model Constants

Table B.1: Constants values (Seavey and Liu, 2009).

Variable	Value	Dimension
$z_{\text{in,TPA}}$	1	n/n
$x_{\text{in,EG}}$	1	n/n
$\varphi_{\text{liq-sol}}$	10^3	$\text{mol s}^{-1}\,\text{m}^{-\frac{9}{2}}$
φ_{vap}	10^{-2}	$\text{mol s}^{-1}\,\text{Pa}^{-0.5}$
$k_{\text{s}}\,A_{\text{sol-liq}}$	1	$\text{m}^3\,\text{s}^{-1}$

Appendix C

GNU Octave Continous reactor code

fun_PETREACTIONS

```
%   _____
%     This function objective is to compute the reaction
%     rates for each specie for PET polymerization.
%
%     Inputs:   NCOMP      – number of components
%               COMPLIST   – list of components
%               TEMP       – reaction temperature (K)
%               LMV        – DIPPR liquid molar volume parameters
%               MOLES      – amount or rate of components (mol or mol/s)
%               VKLIQDENS  – Van Krevelen polymer density parameters
%               MW         – molecular weight parameters (kg/mol)
%               XC         – polymer mole fraction crystals
%
%     Outputs:  DCDT       – reaction rate of species (mol/m3–s)
%               HR         – heat of reaction (J/m3–s)
%
%     Based on the model: Kevin C. Seavey, 2006
%
%     Author: Celia Pedro.
%     Date: Created on February, 2016.
%   _____


    function [ DCDT, HR ] = fun_PETREACTIONS( NCOMP, TEMP, LMV, MOLES, ...
                            XC, VKLIQDENS, MW, COMPLIST )

% pre–allocate memory

  K     = zeros(  8 ) ;
  EQUIL = zeros(  8 ) ;
```

```matlab
    R      = zeros ( 37 )  ;
    PREEXP = zeros (  8 )  ;
    ACTEN  = zeros (  8 )  ;

%

    FOUR   =  4.0    ;
    TWO    =  2.0    ;
    RIDEAL =  8.314  ;
    ZERO   =  0.0    ;


% Enforce limits on temp and moles

    TEMP   = fun_props_LIMITT ( TEMP )  ;

    MOLES  = fun_props_LIMITMOLES ( NCOMP, MOLES )  ;

% Zero out for all components

    DCDT = zeros ( NCOMP, 1 )  ;

% Compute mass fraction

    MASS = fun_phase_MOLETOMASS ( NCOMP, MW, MOLES )  ;

    TOTMASS =  0.D0  ;

    for I = 1 : 6
        TOTMASS = TOTMASS + MASS(I)  ;
    end

    for I = 1 : NCOMP
        MASSFRAC(I)  =  0.D0  ;
    end

    for I = 1 : 6
        MASSFRAC(I) = MASS(I)/TOTMASS  ;
    end

% Compute concentration  (mol/m^3)

    CONC = fun_phase_CONCVOL (NCOMP,TEMP,LMV,MOLES,XC,VKLIQDENS,MW )  ;

% Sort components conscentrations  (mol/kg)

        AA   = ZERO  ;
```

C.2

```
        DEG  = ZERO ;
        EG   = ZERO ;
        TPA  = ZERO ;
        W    = ZERO ;
        BDEG = ZERO ;
        BEG  = ZERO ;
        BTPA = ZERO ;
        TEG  = ZERO ;
        TTPA = ZERO ;
        TVIN = ZERO ;
        TDEG = ZERO ;


        AA   = CONC(1)  ;
        DEG  = CONC(2)  ;
        EG   = CONC(3)  ;
        TPA  = CONC(4)  ;
        W    = CONC(5)  ;
        BDEG = CONC(7)  ;
        BEG  = CONC(8)  ;
        BTPA = CONC(9)  ;
        TEG  = CONC(10);
        TTPA = CONC(11);
        TVIN = CONC(12);
        TDEG = CONC(13);
```

% Calculate segment run concentrations (mol/kg)

```
        SMALL = 1.D-12 ;
        TEGTTPA = TEG*TTPA/(TTPA+BTPA+SMALL) ;
        TEGBTPA = TEG*BTPA/(TTPA+BTPA+SMALL) ;
        BEGTTPA = BEG*TTPA/(TTPA+BTPA+SMALL) ;
        BEGBTPA = BEG*BTPA/(TTPA+BTPA+SMALL) ;
        BTPATVIN = TVIN*BTPA/(TTPA+BTPA+SMALL) ;
        TTPATVIN = TVIN*TTPA/(TTPA+BTPA+SMALL) ;
        TDEGTTPA = TDEG*TTPA/(TTPA+BTPA+SMALL) ;
        TDEGBTPA = TDEG*BTPA/(TTPA+BTPA+SMALL) ;
        BDEGBTPA = BDEG*BTPA/(TTPA+BTPA+SMALL) ;
        BDEGTTPA = BDEG*TTPA/(TTPA+BTPA+SMALL) ;
```

% Calculate rate constants (m^3/mol/s)

```
        for I = 1 : 8
            PREEXP(I) = 0.D0 ;
            ACTEN(I) = 0.D0 ;
            K(I) = 0.D0 ;
            EQUIL(I) = 1.D0 ;
        end
```

```
      PREEXP(1) = 2.08D+03 /60.D0 ;
      PREEXP(2) = 2.08D+03 /60.D0 ;
      PREEXP(3) = 1.76D+02 /60.D0 ;
      PREEXP(4) = 2.22D+08 /60.D0 ;
      PREEXP(5) = 8.32D+04 /60.D0 ;
      PREEXP(6) = 2.50D+05 /60.D0 ;
      PREEXP(7) = 1.14D+05 /60.D0 ;
      PREEXP(8) = 4.77D+07 /60.D0 ;
      ACTEN(1)  = 7.36D+04 ;
      ACTEN(2)  = 7.36D+04 ;
      ACTEN(3)  = 7.74D+04 ;
      ACTEN(4)  = 1.61D+05 ;
      ACTEN(5)  = 1.25D+05 ;
      ACTEN(6)  = 1.25D+05 ;
      ACTEN(7)  = 1.25D+05 ;
      ACTEN(8)  = 1.25D+05 ;
      EQUIL(1)  = 2.50D+00 ;
      EQUIL(3)  = 0.161D+00 ;


      for I = 1 : 8
          K(I) = PREEXP(I)*exp(-ACTEN(I)/RIDEAL/TEMP) ;
      end

% Calculate reactions rates mol/(kg.min)

      R(1)  = FOUR*K(1)*EG*TPA - K(1)/EQUIL(1)*TEGTTPA*W ;
      R(2)  = TWO*K(1)*EG*TTPA - K(1)/EQUIL(1)*TEGBTPA*W ;
      R(3)  = FOUR*K(1)*DEG*TPA - K(1)/EQUIL(1)*TDEGTTPA*W ;
      R(4)  = TWO*K(1)*DEG*TTPA - K(1)/EQUIL(1)*TDEGBTPA*W ;
      R(5)  = TWO*K(2)*TPA*TEG - K(1)/EQUIL(1)*BEGTTPA*W  ;
      R(6)  = K(2)*TEG*TTPA - K(1)/EQUIL(1)*BEGBTPA*W  ;
      R(7)  = TWO*K(2)*TPA*TDEG - K(1)/EQUIL(1)*BDEGTTPA*W  ;
      R(8)  = K(2)*TDEG*TTPA - K(1)/EQUIL(1)*BDEGBTPA*W  ;
      R(9)  = K(1)/EQUIL(1)*TTPATVIN*W ;
      R(10) = K(1)/EQUIL(1)*BTPATVIN*W ;
      R(11) = TWO*K(3)*EG*BEGTTPA - K(3)/EQUIL(3)*TEG*TEGTTPA ;
      R(12) = TWO*K(3)*EG*TDEGTTPA - TWO*K(3)/EQUIL(3)*DEG*TEGTTPA ;
      R(13) = TWO*K(3)*EG*BDEGTTPA - K(3)/EQUIL(3)*TDEG*TEGTTPA ;
      R(14) = TWO*K(3)*EG*BEGBTPA - K(3)/EQUIL(3)*TEG*TEGBTPA ;
      R(15) = TWO*K(3)*EG*TDEGBTPA - TWO*K(3)/EQUIL(3)*DEG*TEGBTPA ;
      R(16) = TWO*K(3)*EG*BDEGBTPA - K(3)/EQUIL(3)*TDEG*TEGBTPA ;
      R(17) = TWO*K(3)*DEG*TEGTTPA - TWO*K(3)/EQUIL(3)*EG*TDEGTTPA ;
      R(18) = TWO*K(3)*DEG*BEGTTPA - K(3)/EQUIL(3)*TEG*TDEGTTPA ;
      R(19) = TWO*K(3)*DEG*BDEGTTPA - K(3)/EQUIL(3)*TDEG*TDEGTTPA ;
      R(20) = TWO*K(3)*DEG*TEGBTPA - TWO*K(3)/EQUIL(3)*EG*TDEGBTPA ;
```

C.4

```
        R(21) = TWO*K(3)*DEG*BEGBTPA − K(3)/EQUIL(3)*TEG*TDEGBTPA ;

        R(22) = TWO*K(3)*DEG*BDEGBTPA − K(3)/EQUIL(3)*TDEG*TDEGBTPA ;

        R(23) = TWO*K(3)*EG*TTPATVIN ;

        R(24) = TWO*K(3)*EG*BTPATVIN ;

        R(25) = TWO*K(3)*DEG*TTPATVIN ;

        R(26) = TWO*K(3)*DEG*BTPATVIN ;

        R(27) = K(3)*TEG*TTPATVIN ;

        R(28) = K(3)*TEG*BTPATVIN ;

        R(29) = K(3)*TDEG*TTPATVIN ;

        R(30) = K(3)*TDEG*BTPATVIN ;

        R(31) = K(4)*BEGBTPA ;

        R(32) = K(5)*TEG*TEGBTPA ;

        R(33) = K(6)*TVIN*TEG ;

        R(34) = K(7)*TEG*TEG ;

        R(35) = TWO*K(7)*TEG*EG ;

        R(36) = FOUR*K(7)*EG*EG ;

        R(37) = K(8)*TEGBTPA ;


% SORT REACTION RATES (MOL/M3−S)


        DCDTPOLY = 0.D0 ;


        for I = 1 : NCOMP
            DCDT(I) = 0.D0 ;
        end
```

```
%               Acetaldehyde
            DCDT(1) = R(9) + R(10) + R(23) + R(24)   ...
                    + R(25) + R(26) + R(27) + R(28) + R(29) + R(30) + R(37) ;


%               Diethylene glycol
            DCDT(2) = −R(3) − R(4) + R(12) + R(15)   ...
                    − (R(17) + R(18) + R(19) + R(20) + R(21) + R(22)) − R(25)   ...
                    − R(26) + R(36) ;


%               Ethylene glycol
            DCDT(3) = −R(1) − R(2) − (R(11) + R(12)   ...
                    + R(13) + R(14) + R(15) + R(16)) + R(17) + R(20)   ...
                    − R(23) − R(24) − R(35) − TWO*R(36) ;


%               Terephthalatic Acid
            DCDT(4) = −R(1) − R(3) − R(5) − R(7)   ...
                    + R(9) ;
```

%   *Water*

```
DCDT(5) = R(1) + R(2) + R(3) + R(4)      ...
          + R(5) + R(6) + R(7) + R(8) - R(9) - R(10)    ...
          + R(34) + R(35) + R(36) ;
```

%   *PET*

```
DCDT(7) = R(7) + R(8) - R(13) - R(16)    ...
          - R(19) - R(22) + R(29) + R(30) + R(33) + R(34) ;
```

%   *B–DEG*

```
DCDT(8) = R(5) + R(6) - R(11)     ...
          - R(14) - R(18) - R(21) + R(27) + R(28) - R(31) ;
```

%   *B–EG*

```
DCDT(9) = R(2) + R(4) + R(6)   ...
          + R(8) - R(10) - R(31) - R(32) - R(37) ;
```

%   *T–TPA*

```
DCDT(10) = R(1) + R(2) - R(5) - R(6) + TWO*(R(11) + R(14))   ...
           + R(12) + R(13) + R(15) + R(16) - R(17) + R(18) - R(20)    ...
           + R(21) + R(23) + R(24) - R(27) - R(28)   ...
           - TWO*R(32) - R(33) - TWO*R(34) - R(35) - R(37) ;

DCDTPOLY = DCDTPOLY + DCDT(10)/2.D0 ;
```

%   *T–EG*

```
DCDT(11) = R(1) - R(2) + R(3) - R(4) + R(5) - R(6) + R(7)   ...
           - R(8) - R(9) + R(10) + R(31) + R(32) + R(37) ;

DCDTPOLY = DCDTPOLY + DCDT(11)/2.D0 ;
```

%   *T–VIN*

```
DCDT(12) = -R(9) - R(10) - (R(23) + R(24) + R(25) + R(26) ...
           + R(27) + R(28) + R(29) + R(30)) + R(31) - R(33) ;

DCDTPOLY = DCDTPOLY + DCDT(12)/2.D0 ;
```

%   *T–DEG*

```
DCDT(13) = R(3) + R(4) - R(7) - R(8) - R(12) + R(13) - R(15) ...
           + R(16) + (R(17) + R(18) + R(19) + R(20) + R(21)   ...
           + R(22)) + R(25) + R(26) - R(29) - R(30) + R(32) ...
           + R(35) ;

DCDTPOLY = DCDTPOLY + DCDT(13)/2.D0 ;
```

C.6

% *Set reaction rate of polymer*

```
        DCDT(6) = DCDTPOLY ;
```

% *Compute heat of reaction (zero)*

```
    HR = 0.D0 ;
```

% *end of file*

% ——
%   *This function computes the key process outputs variables*
%   *for a PET system. The KPOVs are intrinsic viscosity*
%   *(extractables free, dL/g), and the extractables content.*
%
%   *inputs: NCOMP   — number of components*
%   *COMPLIST — component list*
%   *MW   — molecular weight of components (kg/mol)*
%   *MOLES   — amount or flow rate of components (mol or mol/s)*
%
%   *outputs: VISC — intrinsic viscosity (dL/g)*
%   *EXT   — extractables content (mass %)*
%
%   *Based on the model: Kevin C. Seavey, 2006*
%
%   *Author: Celia Pedro.*
%   *Date: Created on February, 2016.*
% ——
    function [VISC EXT] = fun_reactions_PETKPOVS(NCOMP, COMPLIST, MW, MOLES)

%   *Calculate relative viscosity*
    MWN =   fun_props_MWN(NCOMP,MOLES,MW);
    VISC = 2.1D−04 * (1.D3 * MWN)^0.82D0;

%   *Calculate mass of each component (kg)*

    MASS = fun_phase_MOLETOMASS(NCOMP, MW, MOLES);

%   *Calculate total mass (kg) and extractables (%)*
    TOTMASS = 0.D0;

    for I = 1 : 6
        TOTMASS = TOTMASS+ MASS(I);
```

```
        end

    EXT = 0.D0;

    for I = 1 : 5
        EXT = EXT + MASS( I );
    end
    EXT = EXT/TOTMASS * 100.D0;

end
```

C.8

Appendix D

Example of C++ code

Class Pet reactions

```cpp
/*
 * File:    PETREACTIONS.hpp
 * Author:  celia
 *
 * Created on April 27, 2016
 */

#ifndef PETREACTIONS_HPP
#define PETREACTIONS_HPP

#include <math.h>
#include <plantegrity/common/LocalArray.hpp>
#include "parameters.h"
#include "PHASE.hpp"
#include "PROPS.hpp"
//falta chamar props e phase depois

namespace plantegrity {

    template<class T>
    class LocalArray;

    template<class QaDouble>
    class PETREACTIONS {
    public:

        PETREACTIONS() {
        };
```

```
                                                                                
~PETREACTIONS() {
};

void Fun_PETREACTIONS(QaDouble TEMP, QaDouble LMV[][4], QaDouble * MOLES,
        QaDouble XC, QaDouble VKLIQDENS[][6], QaDouble * MW,
        QaDouble * DCDT, QaDouble HR) {



    /*
     * _____
     * _____
     *
     * Kinetics of Kevin C. Seavey, 2006: "Kinetics of PET polymerization −PETREACTIONS
     * Dynamic esterifier"
     * Components:
     * AA
     * DEG
     * EG
     * TPA
     * W
     * PET
     * B−DEG
     * B−EG
     * B−TPA
     * T−EG
     * T−TPA
     * T−VIN
     * T−DEG
     * _____
     * _____
     */


    PROPS<QaDouble> props;
    props.Fun_props_LIMITMOLES(MOLES);
    props.Fun_props_LIMITMOLES(MOLES);
    QaDouble TOTMASS, MASS[Ncomp]; //total mass
    PHASE<QaDouble> phase;
    phase.Fun_phase_MOLETOMASS(MW, MOLES, MASS);

    QaDouble FOUR, TWO, ZERO;
    FOUR = 4.0;
    TWO = 2.0;
    ZERO = 0.0;



    TOTMASS = 0.0;
    for (int i = 0; i < Ncomp; i++) {
```

D.2

```
        TOTMASS = TOTMASS + MASS[ i ];
}


QaDouble MASSFRAC[Ncomp]; // mass fraction of each component
for (int i = 0; i < Ncomp; i++) {
    MASSFRAC[ i ] = 0.0;
}


for (int i = 0; i < 6; i++) {// component 1−6
    MASSFRAC[ i ] = MASS[ i ] / TOTMASS;
}


QaDouble AA(0.0); // component concentrations, mol/kg, 1−5 & 7−13
QaDouble DEG(0.0);
QaDouble EG(0.0);
QaDouble TPA(0.0);
QaDouble W(0.0);
QaDouble BDEG(0.0);
QaDouble BEG(0.0);
QaDouble BTPA(0.0);
QaDouble TEG(0.0);
QaDouble TTPA(0.0);
QaDouble TVIN(0.0);
QaDouble TDEG(0.0);


QaDouble CONC[Ncomp];


phase.Fun_phase_CONCVOL(TEMP, LMV, MOLES, XC, VKLIQDENS, MW, CONC);


AA = CONC[1 − 1];
DEG = CONC[2 − 1];
EG = CONC[3 − 1];
TPA = CONC[4 − 1];
W = CONC[5 − 1];
BDEG = CONC[7 − 1];
BEG = CONC[8 − 1];
BTPA = CONC[9 − 1];
TEG = CONC[10 − 1];
TTPA = CONC[11 − 1];
TVIN = CONC[12 − 1];
TDEG = CONC[13 − 1];



QaDouble SMALL(1e−12); //segments run concentrations, mol/kg
QaDouble TEGTTPA = TEG * TTPA / (TTPA + BTPA + SMALL);
QaDouble TEGBTPA = TEG * BTPA / (TTPA + BTPA + SMALL);
QaDouble BEGTTPA = BEG * TTPA / (TTPA + BTPA + SMALL);
```

```
QaDouble BEGBTPA = BEG * BTPA / (TTPA + BTPA + SMALL);
QaDouble BTPATVIN = TVIN * BTPA / (TTPA + BTPA + SMALL);
QaDouble TTPATVIN = TVIN * TTPA / (TTPA + BTPA + SMALL);
QaDouble TDEGTTPA = TDEG * TTPA / (TTPA + BTPA + SMALL);
QaDouble TDEGBTPA = TDEG * BTPA / (TTPA + BTPA + SMALL);
QaDouble BDEGBTPA = BDEG * BTPA / (TTPA + BTPA + SMALL);
QaDouble BDEGTTPA = BDEG * TTPA / (TTPA + BTPA + SMALL);


QaDouble PREEXP[Ncrate], ACTEN[Ncrate], K[Ncrate], EQUIL[Ncrate];
 // rate constants calculation ,m^3/mol/s
for (int i = 0; i < Ncrate; i++) {
    PREEXP[i] = 0.0;
    ACTEN[i] = 0.0;
    K[i] = 0.0;
    EQUIL[i] = 1.0;
}

PREEXP[1 - 1] = 2.08e3 / 60.0;
PREEXP[2 - 1] = 2.08e3 / 60.0;
PREEXP[3 - 1] = 1.76e2 / 60.0;
PREEXP[4 - 1] = 2.22e8 / 60.0;
PREEXP[5 - 1] = 8.32e4 / 60.0;
PREEXP[6 - 1] = 2.50e5 / 60.0;
PREEXP[7 - 1] = 1.14e5 / 60.0;
PREEXP[8 - 1] = 4.77e7 / 60.0;

ACTEN[1 - 1] = 7.36e4;
ACTEN[2 - 1] = 7.36e4;
ACTEN[3 - 1] = 7.74e4;
ACTEN[4 - 1] = 1.61e5;
ACTEN[5 - 1] = 1.25e5;
ACTEN[6 - 1] = 1.25e5;
ACTEN[7 - 1] = 1.25e5;
ACTEN[8 - 1] = 1.25e5;

EQUIL[1 - 1] = 2.50;
EQUIL[3 - 1] = 0.161;

for (int i = 0; i < Ncrate; i++) {
    K[i] = PREEXP[i] * exp(-ACTEN[i] / Ridealgas / TEMP);
}

// calculate the reaction rates, mol/(kg.min)

QaDouble R[Nrrate];
R[1 - 1] = FOUR * K[1 - 1] * EG * TPA - K[1 - 1] / EQUIL[1 - 1] * TEGTTPA*W;
```

D.4

```
R[2 − 1] = TWO ∗ K[1 − 1] ∗ EG ∗ TTPA − K[1 − 1] / EQUIL[1 − 1] ∗ TEGBTPA∗W;
R[3 − 1] = FOUR ∗ K[1 − 1] ∗ DEG ∗ TPA − K[1 − 1] / EQUIL[1 − 1] ∗ TDEGTTPA∗W;
R[4 − 1] = TWO ∗ K[1 − 1] ∗ DEG ∗ TTPA − K[1 − 1] / EQUIL[1 − 1] ∗ TDEGBTPA∗W;
R[5 − 1] = TWO ∗ K[2 − 1] ∗ TPA ∗ TEG − K[1 − 1] / EQUIL[1 − 1] ∗ BEGTTPA∗W;
R[6 − 1] = K[2 − 1] ∗ TEG ∗ TTPA − K[1 − 1] / EQUIL[1 − 1] ∗ BEGBTPA∗W;
R[7 − 1] = TWO ∗ K[2 − 1] ∗ TPA ∗ TDEG − K[1 − 1] / EQUIL[1 − 1] ∗ BDEGTTPA∗W;
R[8 − 1] = K[2 − 1] ∗ TDEG ∗ TTPA − K[1 − 1] / EQUIL[1 − 1] ∗ BDEGBTPA∗W;
R[9 − 1] = K[1 − 1] / EQUIL[1 − 1] ∗ TTPATVIN∗W;
R[10 − 1]= K[1 − 1] / EQUIL[1 − 1] ∗ BTPATVIN∗W;
R[11 − 1]= TWO ∗ K[3 − 1] ∗ EG ∗ BEGTTPA − K[3 − 1] / EQUIL[3 − 1] ∗ TEG∗TEGTTPA;
R[12 − 1]= TWO ∗ K[3 − 1] ∗ EG ∗ TDEGTTPA − TWO ∗ K[3 − 1] / EQUIL[3 − 1] ∗ DEG∗TEGTTPA;
R[13 − 1]= TWO ∗ K[3 − 1] ∗ EG ∗ BDEGTTPA − K[3 − 1] / EQUIL[3 − 1] ∗ TDEG∗TEGTTPA;
R[14 − 1]= TWO ∗ K[3 − 1] ∗ EG ∗ BEGBTPA − K[3 − 1] / EQUIL[3 − 1] ∗ TEG∗TEGBTPA;
R[15 − 1]= TWO ∗ K[3 − 1] ∗ EG ∗ TDEGBTPA − TWO ∗ K[3 − 1] / EQUIL[3 − 1] ∗ DEG∗TEGBTPA;
R[16 − 1]= TWO ∗ K[3 − 1] ∗ EG ∗ BDEGBTPA − K[3 − 1] / EQUIL[3 − 1] ∗ TDEG∗TEGBTPA;
R[17 − 1]= TWO ∗ K[3 − 1] ∗ DEG ∗ TEGTTPA − TWO ∗ K[3 − 1] / EQUIL[3 − 1] ∗ EG∗TDEGTTPA;
R[18 − 1]= TWO ∗ K[3 − 1] ∗ DEG ∗ BEGTTPA − K[3 − 1] / EQUIL[3 − 1] ∗ TEG∗TDEGTTPA;
R[19 − 1]= TWO ∗ K[3 − 1] ∗ DEG ∗ BDEGTTPA − K[3 − 1] / EQUIL[3 − 1] ∗ TDEG∗TDEGTTPA;
R[20 − 1]= TWO ∗ K[3 − 1] ∗ DEG ∗ TEGBTPA − TWO ∗ K[3 − 1] / EQUIL[3 − 1] ∗ EG∗TDEGBTPA;
R[21 − 1]= TWO ∗ K[3 − 1] ∗ DEG ∗ BEGBTPA − K[3 − 1] / EQUIL[3 − 1] ∗ TEG∗TDEGBTPA;
R[22 − 1]= TWO ∗ K[3 − 1] ∗ DEG ∗ BDEGBTPA − K[3 − 1] / EQUIL[3 − 1] ∗ TDEG∗TDEGBTPA;
R[23 − 1]= TWO ∗ K[3 − 1] ∗ EG∗TTPATVIN;
R[24 − 1]= TWO ∗ K[3 − 1] ∗ EG∗BTPATVIN;
R[25 − 1]= TWO ∗ K[3 − 1] ∗ DEG∗TTPATVIN;
R[26 − 1]= TWO ∗ K[3 − 1] ∗ DEG∗BTPATVIN;
R[27 − 1]= K[3 − 1] ∗ TEG∗TTPATVIN;
R[28 − 1]= K[3 − 1] ∗ TEG∗BTPATVIN;
R[29 − 1]= K[3 − 1] ∗ TDEG∗TTPATVIN;
R[30 − 1]= K[3 − 1] ∗ TDEG∗BTPATVIN;
R[31 − 1]= K[4 − 1] ∗ BEGBTPA;
R[32 − 1]= K[5 − 1] ∗ TEG∗TEGBTPA;
R[33 − 1]= K[6 − 1] ∗ TVIN∗TEG;
R[34 − 1]= K[7 − 1] ∗ TEG∗TEG;
R[35 − 1]= TWO ∗ K[7 − 1] ∗ TEG∗EG;
R[36 − 1]= FOUR ∗ K[7 − 1] ∗ EG∗EG;
R[37 − 1]= K[8 − 1] ∗ TEGBTPA;


QaDouble DCDTPOLY; // for comptype==4 (octave programe)
DCDTPOLY = 0.0;


for (int i = 0; i < Ncomp; i++) {
    DCDT[i] = 0.0;
}


DCDT[1 − 1] = R[9 − 1] + R[10 − 1] + R[23 − 1] + R[24 − 1]
        + R[25 − 1] + R[26 − 1] + R[27 − 1] + R[28 − 1] + R[29 − 1] + R[30 − 1]
        + R[37 − 1];
```

DCDT[2 − 1] = −R[3 − 1] − R[4 − 1] + R[12 − 1] + R[15 − 1]
   − (R[17 − 1] + R[18 − 1] + R[19 − 1] + R[20 − 1] + R[21 − 1] + R[22 − 1])
   − R[25 − 1]

   − R[26 − 1] + R[36 − 1];

DCDT[3 − 1] = −R[1 − 1] − R[2 − 1] − (R[11 − 1] + R[12 − 1]
   + R[13 − 1] + R[14 − 1] + R[15 − 1] + R[16 − 1]) + R[17 − 1] + R[20 − 1]
   − R[23 − 1] − R[24 − 1] − R[35 − 1] − TWO * R[36 − 1];

DCDT[4 − 1] = −R[1 − 1] − R[3 − 1] − R[5 − 1] − R[7 − 1]
   + R[9 − 1];

DCDT[5 − 1] = R[1 − 1] + R[2 − 1] + R[3 − 1] + R[4 − 1]
   + R[5 − 1] + R[6 − 1] + R[7 − 1] + R[8 − 1] − R[9 − 1] − R[10 − 1]
   + R[34 − 1] + R[35 − 1] + R[36 − 1];

DCDT[7 − 1] = R[7 − 1] + R[8 − 1] − R[13 − 1] − R[16 − 1]
   − R[19 − 1] − R[22 − 1] + R[29 − 1] + R[30 − 1] + R[33 − 1] + R[34 − 1];

DCDT[8 − 1] = R[5 − 1] + R[6 − 1] − R[11 − 1]
   − R[14 − 1] − R[18 − 1] − R[21 − 1] + R[27 − 1] + R[28 − 1] − R[31 − 1];

DCDT[9 − 1] = R[2 − 1] + R[4 − 1] + R[6 − 1]
   + R[8 − 1] − R[10 − 1] − R[31 − 1] − R[32 − 1] − R[37 − 1];

DCDT[10 − 1] = R[1 − 1] + R[2 − 1] − R[5 − 1] − R[6 − 1] + TWO * (R[11 − 1] + R[14 − 1])
   + R[12 − 1] + R[13 − 1] + R[15 − 1] + R[16 − 1] − R[17 − 1] + R[18 − 1]
   − R[20 − 1]
   + R[21 − 1] + R[23 − 1] + R[24 − 1] − R[27 − 1] − R[28 − 1]
   − TWO * R[32 − 1] − R[33 − 1] − TWO * R[34 − 1] − R[35 − 1] − R[37 − 1];

DCDTPOLY = DCDTPOLY + DCDT[10 − 1] / 2.0;

DCDT[11 − 1] = R[1 − 1] − R[2 − 1] + R[3 − 1] − R[4 − 1] + R[5 − 1] − R[6 − 1]
   + R[7 − 1]
   − R[8 − 1] − R[9 − 1] + R[10 − 1] + R[31 − 1] + R[32 − 1] + R[37 − 1];

DCDTPOLY = DCDTPOLY + DCDT[11 − 1] / 2.0;

DCDT[12 − 1] = −R[9 − 1] − R[10 − 1] − (R[23 − 1] + R[24 − 1] + R[25 − 1] + R[26 − 1]
   + R[27 − 1] + R[28 − 1] + R[29 − 1] + R[30 − 1]) + R[31 − 1] − R[33 − 1];

D.6

```
        DCDTPOLY = DCDTPOLY + DCDT[12 − 1] / 2.0;



        DCDT[13 − 1] = R[3 − 1] + R[4 − 1] − R[7 − 1] − R[8 − 1] − R[12 − 1] + R[13 − 1]
                − R[15 − 1]
                + R[16 − 1] + (R[17 − 1] + R[18 − 1] + R[19 − 1] + R[20 − 1] + R[21 − 1]
                + R[22 − 1]) + R[25 − 1] + R[26 − 1] − R[29 − 1] − R[30 − 1] + R[32 − 1]
                + R[35 − 1];


        DCDTPOLY = DCDTPOLY + DCDT[13 − 1] / 2.0;



        DCDT[6 − 1] = DCDTPOLY; // reaction rate of the polymer

        HR = 0.0; // heat reaction = zero

}

    void Fun_reactions_PETKPOVS(QaDouble ∗ MW, QaDouble ∗ MOLES, QaDouble ∗ VISC,
            QaDouble EXT) {

        /∗
         ∗ This function computes the key process outputs variables
         ∗ for a PET system. The KPOVs are intrinsic viscosity
         ∗ (extractables free, dL/g), and the extractables content.
         ∗
         ∗ inputs:
           MW        − molecular weight of components (kg/mol)
           MOLES     − amount or flow rate of components (mol or mol/s)
         ∗
         ∗ outputs:
           VISC  − intrinsic viscosity (dL/g)
           EXT   − extractables content (mass %)
         ∗
         ∗/

        QaDouble MWN, TEMP;
        PROPS<QaDouble> mwn(TEMP);
        mwn.Fun_props_MWN(MOLES, MW, MWN);

        VISC = 2.1e−4 ∗ pow((1e3 ∗ MWN), 0.82); // relative viscosity

        QaDouble MASS;
        PHASE<QaDouble> moletomass(MOLES);
        moletomass.Fun_phase_MOLETOMASS(MOLES, MW, MASS);

        QaDouble TOTMASS = 0.0;
```

```
            for ( int  i  =  0;  i  <  6;  i++) {
                TOTMASS  +=  MASS[ i ];
            }
            EXT  =  0 . 0;

            for ( int  i  =  0;  i  <  5;  i++) {
                EXT  =  EXT  +  MASS[ i ];
            }
            EXT  =  EXT  /  TOTMASS  *  100.0;


        }
    };
}
#endif /* PETREACTIONS_HPP */
```

D.8